FINAL REPORT

Project Title: S3 Deck Unit Bridge Deck Analysis under Live Load 2013/14 to 2016/17 - Years 1-4

ARRB Project No: PRG16022

Author/s: Hanson Ngo & Giovanna Zanardo

Client: Queensland Department of Transport and Main Roads

Date: August 2017

TC-710-4-4-8

AN INITIATIVE BY:

SUMMARY

Project Purpose

The four-year project undertook comprehensive investigations into the performance of deck unit (DU) bridges. DU bridges comprise simply-supported spans of rectangular prestressed concrete hollow units, tied by transverse stressing bars (TSBs). Standard numerical assessment of DU bridges has flagged inadequate capacity, while no significant signs of distress have been identified. The project was, therefore, carried out to address the disparities between theoretical assessments and the actual behaviour of this bridge type. In particular, the project's test program included: load testing of DU bridges in operational condition (Year 1); assessment of the ultimate capacity of individual DUs and kerb units (KUs) (Year 2); performance and ultimate load testing of a partial DU bridge re-assembled from salvaged DUs in a laboratory (Year 3 and Year 4). An additional task was undertaken on a real-life DU bridge to investigate the effects of TSB damage on the structural performance of the bridge (Year 4).

Project Findings

As part of Year 1, in-service monitoring and performance load testing were conducted on Canal Creek Bridge (east of Cloncurry, Queensland). The bridge is a two-span simply-supported DU bridge built in 1970, with decks that consist of 13 DUs, 8.3 m long between supports. The results showed that the bridge superstructure performed better than theoretically predicted. The load transfer mechanism of the tested deck was found to be similar to that of a flat slab bridge. These results are critical to calibrate existing numerical models, mostly based on grillage analysis, as well as to refine standard capacity assessment procedures.

During Year 2, destructive testing of individual units, both in bending and shear was conducted at the Structures Laboratory of the University of Queensland (UQ). The 9.1-m-long test units provided a significant sample of DUs used for bridges built in the 1970s. These bridges comprise inner DUs with a low depth and inadequate shear reinforcement, and upright KUs with a significantly higher stiffness. All the salvaged deck and KUs exhibited bending and shear capacities higher than those estimated from design specifications. The DUs achieved a primarily ductile failure, while the KUs failed in a more brittle manner after sudden cracking. Further, concrete and steel cores yielded material strengths higher than the design values assumed for structural assessment.

A partial DU bridge was re-assembled and tested at the UQ Structures Laboratory in Year 3. The test bridge included six 8.3 m long DUs and one KU, which were salvaged from a decommissioned bridge. The performance load tests provided results consistent with the site tests conducted during Year 1, as the Canal Creek Bridge was built with units of similar design. In fact, the bending performance of the test bridge appeared to reproduce that of a concrete slab. In the destructive test, the KU was the first structural element to fail in bending. The failure mode of the test bridge was predominantly ductile. There was a minimal load re-distribution between the KU and the DUs at failure. The load distribution factor (LDF) derived for the DUs remained mostly unaltered across different load tests and up to failure.

To investigate the effects of TSB damages on the performance of DU bridges, additional testing was conducted in Year 4 as a variation to the

original project scope on Sandgate Road Bridge. This bridge, which carries the Gateway Motorway across Sandgate Road in Boondall (Brisbane), consists of 10 simply-supported spans, with 15 DUs in each span transversely tied by TSBs at 2 m spacing. The behaviour of 16 m long span 9 was investigated via both in-service monitoring and controlled load tests. The damage to the TSBs was gradually introduced by severing the TSBs at the pre-defined locations in incremental stages. Data from the load tests show that extensive TSB damage leads to an 18% increase of the LDF, a 32% strain increase, and a 30% increase of vertical deflections. On the other hand, the maximum LDF associated with the deck response after TSB severing matches the maximum LDF measured under random traffic. Based on the variation of the position of the neutral axis, TSB damage can result in an 18% reduction of the load-carrying capacity of the overall superstructure.

Conclusions

The findings of this project have provided an improved understanding of how DU bridges behave. It is critical for TMR and its network operations in making informed decisions on the restrictions on heavy vehicle movements, as well as on implementing strengthening/maintenance measures or planning bridge replacement.

The field data collected is valuable for the development of a calibrated computer model which can be used to more accurately estimate the capacity of DU bridges. The calibration process is going to be realised through another NACoE project in 2017/18.

ACKNOWLEDGEMENTS

The authors would like to acknowledge the assistance and support provided by a number of staff of TMR Structures Engineering & Technology team. In addition, the contribution of the technical staff at the Structures Laboratory at the University of Queensland is gratefully acknowledged.

CONTENTS

TABLES

FIGURES

1 INTRODUCTION

1.1 Background

The Queensland Department of Transport and Main Roads (TMR) has been investigating viable options for the effective management of the state transport infrastructure, which includes approximately 3000 bridges and 4000 culverts. Since 2014, TMR has been working jointly with ARRB on a number of research projects on asset management, specifically within the National Asset Centre of Excellence (NACOE), a research framework funded by the Queensland Government. The NACOE multi-year research program covers areas of strategic interest in network operation and performance, including the development of efficient methodologies for the assessment of existing bridge structures along heavy vehicle routes.

More than 1900 DU bridges have been built in Queensland since the 1960s, which correspond to more than 60% of TMR bridge assets. The majority of DU bridges are transversely post-tensioned via transverse stressing bars (TSBs). This bridge type includes upright external deck units as kerbs (or kerb units, KUs), while the absence of shear-keys leads to a load transfer mechanism that entirely relies on the mortar joints between adjacent units and the transverse compression of the TSBs. Standard numerical assessments of DU bridges indicate inadequate capacity, although no major concrete cracking or other significant signs of superstructure distress have been highlighted by regular close-up investigations and Level 2 inspections.

While most DU bridges are assessed via grillage analysis, the development of more accurate numerical models of the superstructure requires parameter tuning and calibration via comprehensive site measurements of the behaviour of all superstructure components. To make grillage models sufficiently representative of the real-life structure, the roles of the stiffer KUs, the mortar joints, and of the TSBs in transferring the load between the DUs invoke the need for fine tuning of critical parameters, such as the transverse stiffness and torsional inertia.

In detail, in accordance with the grillage analogy, the numerical representation of a bridge deck can be simplified via a grid of longitudinal and transverse elements. In the case of DU bridges, the grid of longitudinal elements is usually defined by the properties of each DU/KU. However, the definition of the transverse elements, which would have to account for the TSBs and any transverse connection between the beams, is still under debate. In addition, as the KUs are significantly stiffer than the internal DUs, it has been observed in the theoretical models that the KUs attract a greater portion of the load applied on the superstructure, which can lead to overstressing of these units before the internal DUs mobilise their full strength.

It is anticipated that the outcomes from the project are likely to lead to significant savings in terms of asset management of DU bridges. An improved understanding of the actual performance of these bridges under operational loads will translate into more effective planning of maintenance/strengthening measures and a likely deferment of bridge replacement. In detail, the following benefits can be realised:

- Restrictions on existing DU bridges, especially on heavy vehicle routes (e.g. Flinders Highway) will be reviewed to allow increased freight movement. An improved freight movement is correlated with economic benefits and, in turn, increased productivity.
- Strengthening measures and planned replacement of the superstructure of a number of DU bridges will no longer be necessary.
- The costs attached to consultant contracts, to carry out detailed load rating and numerical assessment of DU bridges will be reduced.
- The gained understanding of the performance of DU bridges will lead to improved risk management, especially in terms of identification of potential damage induced by heavy vehicles and, thus, effective prevention measures.

In addition, the project would provide invaluable knowledge in terms of:

- methods and procedures for bridge monitoring and testing to failure, both in the laboratory and in operational conditions
- industry collaborations across various sectors (e.g. freight industry, universities, consultants) on key technologies for bridge monitoring and asset management
- TMR and ARRB coordinated work for the development of large-scale research projects.

This project targets the application of cutting-edge technologies and research methods, which are the core of the innovation that TMR is fostering under the NACOE agreement.

1.2 Details of the Research Program

The multi-year test program started in mid-2013 and was delivered over four years. A variation of the original scope was made in early 2017 to include additional field testing of a DU bridge. The overall program was developed with the following timeline:

- Year 1 – Project scoping and literature review, followed by the development of the instrumentation and long-term program for bridge load testing and monitoring, including the design and implementation of performance testing of an in-service bridge
- Year 2 – Laboratory testing of individual DUs and KUs taken from decommissioned bridges
- Year 3 and Year 4 – Load testing up to failure of a partial DU bridge re-assembled in a laboratory from salvaged units, including one KU and six DUs
- Year 4 (Variation) – In-service monitoring and load testing of one span of a real-life DU bridge, before and after the introduction of incremental TSB damage.

1.3 Aims

The aims of the project were to develop:

- effective instrumentation for reliable measurements of the performance of prestressed beams and superstructures, such as DU bridges
- in-service monitoring plans and load testing procedures for DU bridges
- guidelines for the development and calibration of numerical models of DU bridges, as well as for the assessment of the structural capacity.

1.4 Scope

The four-year scope of works, including the variation implemented in the second half of the fourth year, covered the following tasks:

- definition of the main milestones, and steps required to achieve them
- definition of project hold points and agreements to proceed with the program
- comparison of available budget and resources with project requirements and schedule
- formation of a collaboration and core working group
- review of existing practices both in terms of structural assessment, testing and analytical/numerical modelling
- selection of viable local laboratories and resources for structural testing
- identification of critical heavy-vehicle routes and, thus, of candidate structures for testing
- resourcing of salvaged beams for comprehensive laboratory testing

- investigations on the contribution of TSBs to the overall deck capacity.

1.4.1 Year 1 – Literature Review, Instrumentation, and Site Testing

The Year 1 program included the following tasks prior to bridge testing:

- detailed scoping of all stages of the project
- literature review
- selection of a specific bridge for short-term monitoring and load testing
- preparation of the testing program for an in-service bridge
- engagement of the preferred supplier of testing equipment
- development of numerical models to assess the deck behaviour
- delivery of a summary report.

Site testing required the following tasks:

- instrumenting the selected in-service bridge
- implementation of static and dynamic load tests, as well as short-term condition monitoring
- delivery of a report detailing the testing and results.

1.4.2 Year 2 – Laboratory Testing of Individual Deck and Kerb Units

The Year 2 program included the following tasks:

- definition of scope for the laboratory tests, i.e. methodology and targeted outcomes
- retrieval of KUs and DUs as a significant sample of DU bridges
- sensor system design
- testing design both for bending and shear tests
- selection and engagement of the preferred laboratory
- preparation of the testing program with load tests up to failure
- execution of all planned tests up to structural failure
- data processing and analysis (including derivation of ultimate bending, shear, and torsional capacities of all tested units)
- delivery of a report detailing the laboratory testing and results.

1.4.3 Year 3 and Year 4 – Laboratory Testing of a Partial DU Bridge

The Year 3 program included the following tasks:

- definition of scope for the laboratory tests, i.e. methodology and targeted outcomes
- selection of KUs and DUs for the partial DU bridge (inclusive of the selection between new prefabricated DUs and DUs salvaged from decommissioned bridges)
- construction of the test structure from salvaged DUs and one KU
- sensor system design
- testing design both for bending and shear tests
- preparation of the testing program with load tests up to failure
- execution of all planned tests up to structural failure

- data processing and analysis (including derivation of ultimate bending, shear, and torsional capacity of the test structure)
- delivery of a report detailing the laboratory testing and results.

1.4.4 Year 4 (Variation) – Load Testing of Sandgate Bridge

An opportunity arose for further testing of a real-life DU bridge when Sandgate Road Bridge was planned for demolition as part of the Gateway Upgrade North project. A testing program was developed and included in the project. This testing program included the following tasks:

- definition of scope for the site tests, i.e. methodology and targeted outcomes
- sensor system design, including development of ad hoc data acquisition and archiving systems for long-term condition monitoring and extended load tests
- definition of testing methodology, including sequence of TSB damaged stages, vehicle loads and paths for static tests
- bridge instrumentation, including surface preparation and method statement to access the superstructure
- execution of load tests and implementation of the testing sequence, based on the instantaneous output from all sensors
- data processing and analysis (including statistics of traffic data, analysis of the load distribution factor and neutral axis position for all beams)
- delivery of a report detailing the condition monitoring and load testing results.

1.5 Outline of the Final Report

This report presents a summary of the results obtained from the four-year program, as outlined in Sections 1.4.1–1.4.4 for Years 1–4, including:

- literature review, instrumentation, and site testing (Canal Creek Bridge, Flinders Highway)
- laboratory testing of individual DUs and KUs
- Year 3 and Year 4 – laboratory testing of a partial DU bridge
- Year 4 (variation) – condition monitoring of an in-service bridge and load testing under incremental TSB damage (Sandgate Rd Bridge, Gateway Motorway).

The detailed analysis and results, as obtained from each stage of the program, are discussed in the following reports:

- *S3: Deck unit bridge deck analysis under live load – year 1 report* (Ngo, Kotze, & Pape 2014)
- *BIS 7703 Canal Creek Bridge: load test and in-service monitoring* (Ngo & Pape 2015)
- *S3: Deck unit bridge deck analysis under live load – year 2 report* (destructive testing of deck units in shear and bending) (Ngo, Pape & Kotze 2015)
- *S3: Deck unit bridge deck analysis under live load – year 3 report:* (load test of a full-scale transversely stressed DU bridge in laboratory) (Ngo 2017).
- *GUN – Sandgate Rd Bridge load testing report* (Ngo & Zanardo 2017).

The bibliographic details of each report are given in the references section.

2 LITERATURE REVIEW

2.1 Approaches and Models for Structural Assessment

As the DU bridge type is unique to Queensland, there is a scarcity of published literature on relevant design and assessment methodologies. The unique features of DU bridges include:

- The beams have smooth sides (no shear-keys) thus transverse post-tensioned bars and friction are critical for load transfer between adjacent units. The gaps between the units are filled with mortar prior to the deck being transversely post-tensioned.
- The level of prestress transversely is low in comparison with the longitudinal prestress.
- DUs have nominal or no shear reinforcement.
- The deck wearing surface (DWS) is generally asphalt i.e. there is no concrete overlay.
- KUs are either cast-in situ or precast, and are significantly stiffer than the internal DUs.

Methodologies for capacity assessment and numerical modelling have been developed for similar structures, such as precast prestressed DU bridges with transverse stressing bars and shear-keys, or with a concrete overlay. These methodologies are summarised below.

2.1.1 Numerical Models of the Transverse Load Distribution in Multi-beam Bridges

Hulsbos (1962) developed a theoretical and experimental investigation on the lateral distribution of wheel loads on multi-beam bridges with or without shear-keys, and with lateral bolts that may or may not be prestressed. The theoretical investigation is based on the theory of orthotropic plates. However, as the stiffness in the transverse direction is dependent on the efficiency of the shear-keys and lateral bolts, should slippage occur between adjacent beams, deflection and stress distribution do not follow the rules of plate theory. Therefore, empirical approximation is used to evaluate the change of the internal forces.

It was assumed that the ratio between longitudinal stiffness and lateral stiffness is not constant. It varies along the bridge and it is dependent on the magnitude and location of the applied load as well as the level of transverse prestressing. A parameter α, which is the ratio between longitudinal bending stiffness and transverse bending stiffness, is introduced. For an isotropic and homogeneous plate, α = 1. For longitudinal beams connected side-by-side by continuous hinges, α = 0 as the transverse bending stiffness is zero. For other immediate conditions α will vary between 0 and 1. From experimental results, α is expressed as a function of the (total) transverse post-tensioning force, F and the load applied at the centre (P_c) or edge (P_e) of the bridge, as follows (Equation 1):

For a centre load: $\propto = 0.23\sqrt{F/P_c}$ (1)

For an edge load: $\propto = 0.1\sqrt[3]{F/P_e}$

Where the theoretical and experimental deflections are in good agreement, then the moments in the beams could be calculated by the theory of orthotropic plates. The parameter α was determined by matching the measured with the theoretical deflection distributions, in which the theoretical deflections of the beams were calculated as a function of α using the theory of orthotropic plates.

This method has potential in determining a stiffness ratio between transverse and longitudinal members for use in the simple grillage model, based on matching of beam deflections measured from static field testing with those obtained from grillage models using various values of α.

However, α should be related to some parameters that are easy to implement rather than a ratio between F and P.

2.1.2 CIRIA Recommendations on Grillage Analysis for Pseudo-slab Bridge Decks

West (1973) presented a simple grillage model, in which the stiffness of longitudinal and transverse members is calculated based on the full cross-section (Figure 2.1).

This method does not take into account the effects of transverse stressing bars or the behaviour of the interface between beams.

Figure 2.1: Example of grillage model of a DU bridge with prestressed diaphragms

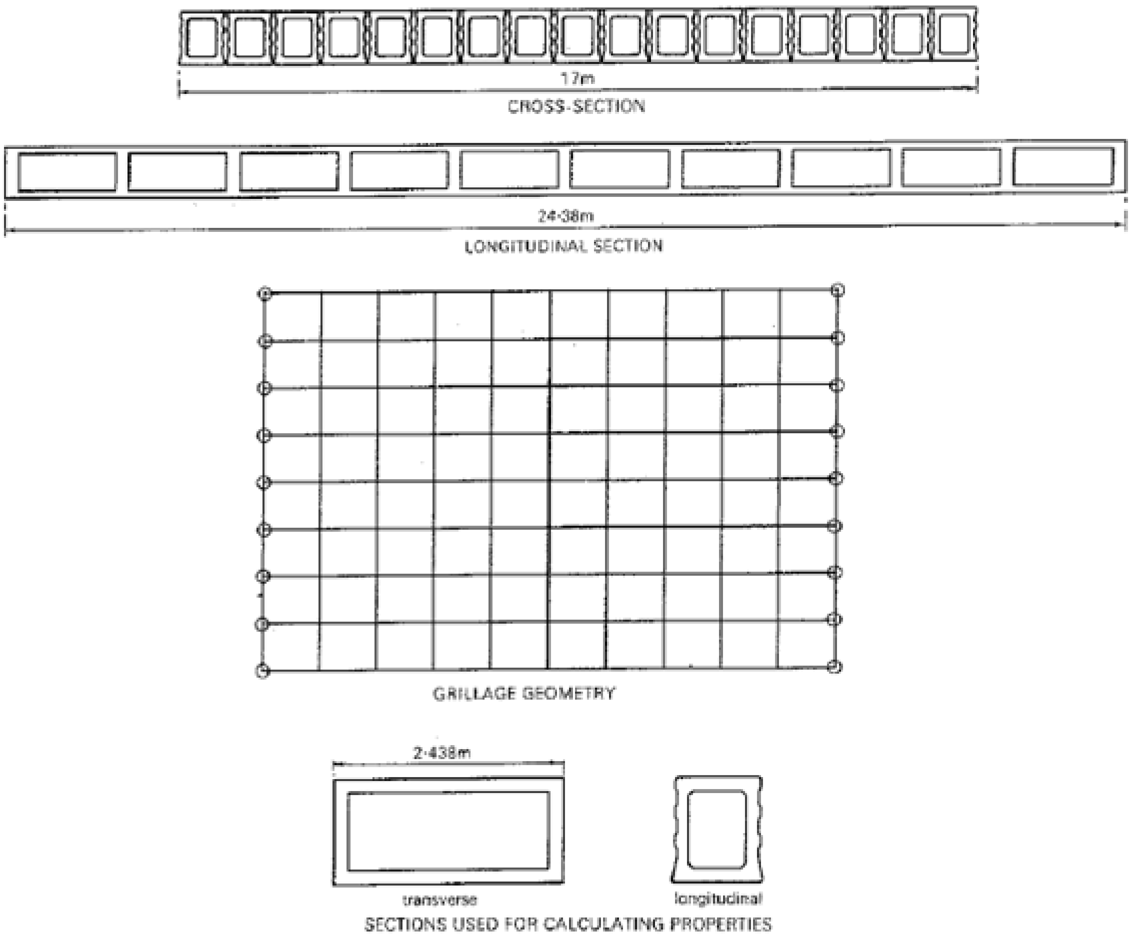

Source: West (1973).

2.1.3 Grillage Models for Flat Slabs, Slab-on-girder Bridges, and Girder Bridges

Hambly (1991) discussed various options for modelling a shear-key slab with a grillage (Figure 2.2a). In one of the recommended grillage options, the stiff outriggers are used to transfer transverse loads from the centreline to the edges of the longitudinal shear-keys. If the shear-keys do not have any bending stiffness then the connection between outriggers can be modelled using a pin connection (Figure 2.2b). When a shear-key does have bending stiffness, the outriggers can be connected via short flexible members, so as to simulate the bending stiffness of the shear-key (Figure 2.2c). The length and stiffness of the flexible connections should match the length and stiffness of the shear-keys.

Figure 2.2: Modelling shear-key slab by grillage simulation

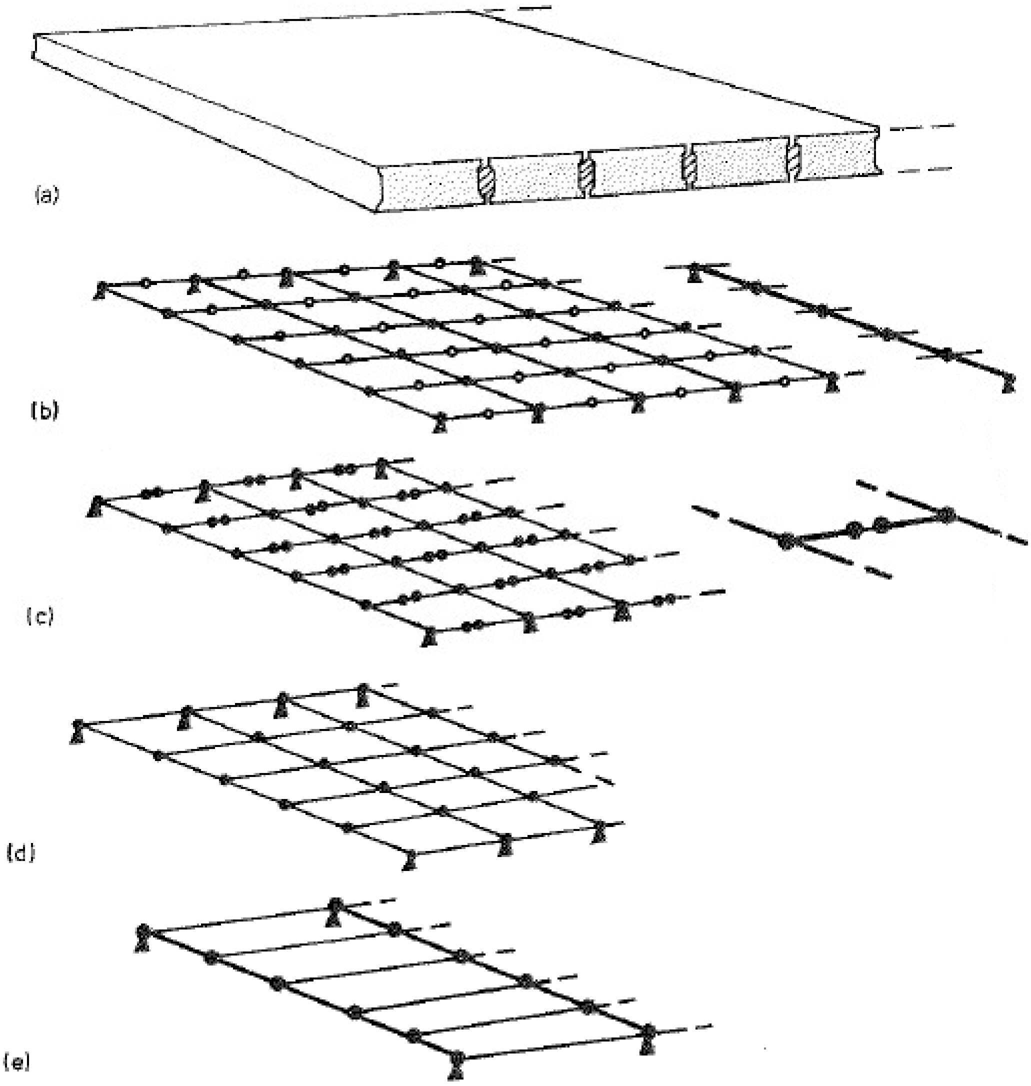

Source: Hambly (1991).

The number of grillage members can be reduced by replacing a group of transverse elements of varying stiffness with a single member of equivalent stiffness (Figure 2.2d), or by replacing two or more beams with one single longitudinal member (Figure 2.2e). To further reduce the computing resources, a series of transverse members of varying stiffness can be simplified by a single member of equivalent stiffness (Equation 2 and Figure 2.3):

$$\frac{M}{\theta} = \frac{2}{\int \frac{dx}{EI}} = \frac{2}{\frac{l-a}{E_1 I_1} + \frac{a}{E_2 I_2}} = \frac{2}{\frac{I}{E_e I_e}} \qquad 2$$

where

M = transverse bending moment

θ = rotation of the DU at the centreline

E = Young's modulus

I = moment of inertia

E_1 = Young's modulus of the first section in the chain

I_1 = moment of inertia of the first section in the chain

E_2 = Young's modulus of the second section in the chain

I_2 = moment of inertia of the second section in the chain

E_e = Young's modulus of the equivalent member

I_e = moment of inertia of the equivalent member

Figure 2.3: Representation of a chain of members with different properties by an equivalent uniform grillage member

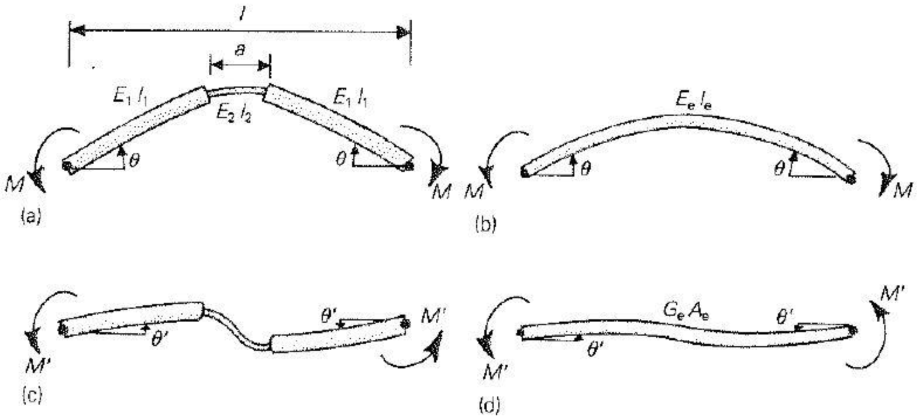

Source: Hambly (1991).

It should be noted that the equivalent method described in Figure 2.3 cannot be used for DU bridges without shear-keys. In this case or when the flexural stiffness of the shear-key is low, Equation 2 becomes indeterminate. If such a scenario was suggested, a pin joint should be placed as a connection between the longitudinal elements.

Further, the proposed methods by Hambly (1991) do not account for the effects of transverse post-tensioning, which has the primary function of increasing the transverse bending stiffness.

2.1.4 Numerical Models for Girder Bridges

According to Buckle (1984), the methods listed in Table 2.1 can be used to analyse multi-beam bridges, together with the folded plate, finite strip and finite element methods.

Table 2.1: Typical analysis methods for multi-beam bridges

Shear-key model	Analysis method	Description
Single point hinge	Transfer matrix, direct stiffness	Simplified discrete beam methods
Multiple point hinges	Direct stiffness	Equivalent grid methods
Continuous hinge line	Matrix force	Refined discrete beam methods
Pseudo plate	Classical plate theory	Equivalent plate methods

Source: Buckle (1984).

Note: 'Equivalent grid methods' are the grillage modelling approaches.

According to Buckle's approach to grillage analysis, the deck is divided into a number of transverse strips that act as transverse members. The longitudinal beams are interconnected by these transverse members at a discrete number of points. The equivalent stiffness of each strip is determined by taking into account the transverse bending stiffness, the near-rigid shear stiffness, as well as the axial and torsional actions. As a result, the transverse connectors transfer only vertical shear forces and torsional moments about the normal axis to the shear-key. The flexural moment about the shear-key centreline is zero.

The equivalent transverse members should be defined as in the following options:

1. *Continuous beam elements of low flexural stiffness* – Since low flexural stiffness results in the reduction of both the flexural moments and shear forces, this option does not allow the accurate quantification of the shear force distribution in the transverse direction (Figure 2.4a).
2. *Discontinuous beam elements interconnected by vertical almost-rigid springs* – The stiffness of the spring can be adjusted to simulate elastic deformations of the shear-keys. In case such deformations are negligible, a non-zero value can be manually specified (Figure 2.4b). However, an excessively large value associated with the shear-key deformations may result in numerical instabilities or non-converging solutions of the system equations.
3. *Discontinuous beam elements interconnected by horizontal torsionless bars* – Similarly to Option 2, very rigid links or 'bars' are introduced to avoid possible numerical instabilities (Figure 2.4c).
4. *Continuous beam elements with flexural pins* – As the transverse elements have flexural and torsional stiffness, the pin is position to match the location of the shear-key. This representation reproduces the shear transfer and zero transverse moment conditions (Figure 2.4d).
5. *Modified longitudinal beam element* – A special H-shape element representing both longitudinal and transverse members is defined (Figure 2.4e), with four vertical displacements (at nodes e, d, l, and m) and two rotations (at nodes f and n).

These above options are all applicable to girder bridges with shear-keys. However, similarly to the methods proposed by Hambly (1991), the effects of transverse post-tensioning are not taken into account.

Badwan and Liang (2007) implemented the Hambly (1991) method for bridge decks with prestressed girders, where equivalent transverse members from grillage models are used to determine the required level of transverse post-tensioning. The required post-tensioning stress per unit length of the span is calculated based on the maximum transverse bending moment, half thickness of the deck, and the moment of inertia of the equivalent transverse grillage member. The properties of the grout material and the dimensions of the shear-key were taken into account in calculating the sectional properties of the equivalent transverse members. The analysis assumes that the grouted joint has little transverse torsional stiffness. Thus the torsional constant of the transverse members is calculated based on the transverse stiffness of concrete only, and is taken as $D^3/6$ per unit length, where D is the thickness of the precast concrete beam.

This Badwan and Liang method however is primarily applicable to girders that are transversely joined via shear-keys. For DU bridges that lack shear-keys, a pin joint can be used between adjacent longitudinal elements as suggested by Hambly (1991).

Figure 2.4: Alternative equivalent transverse members

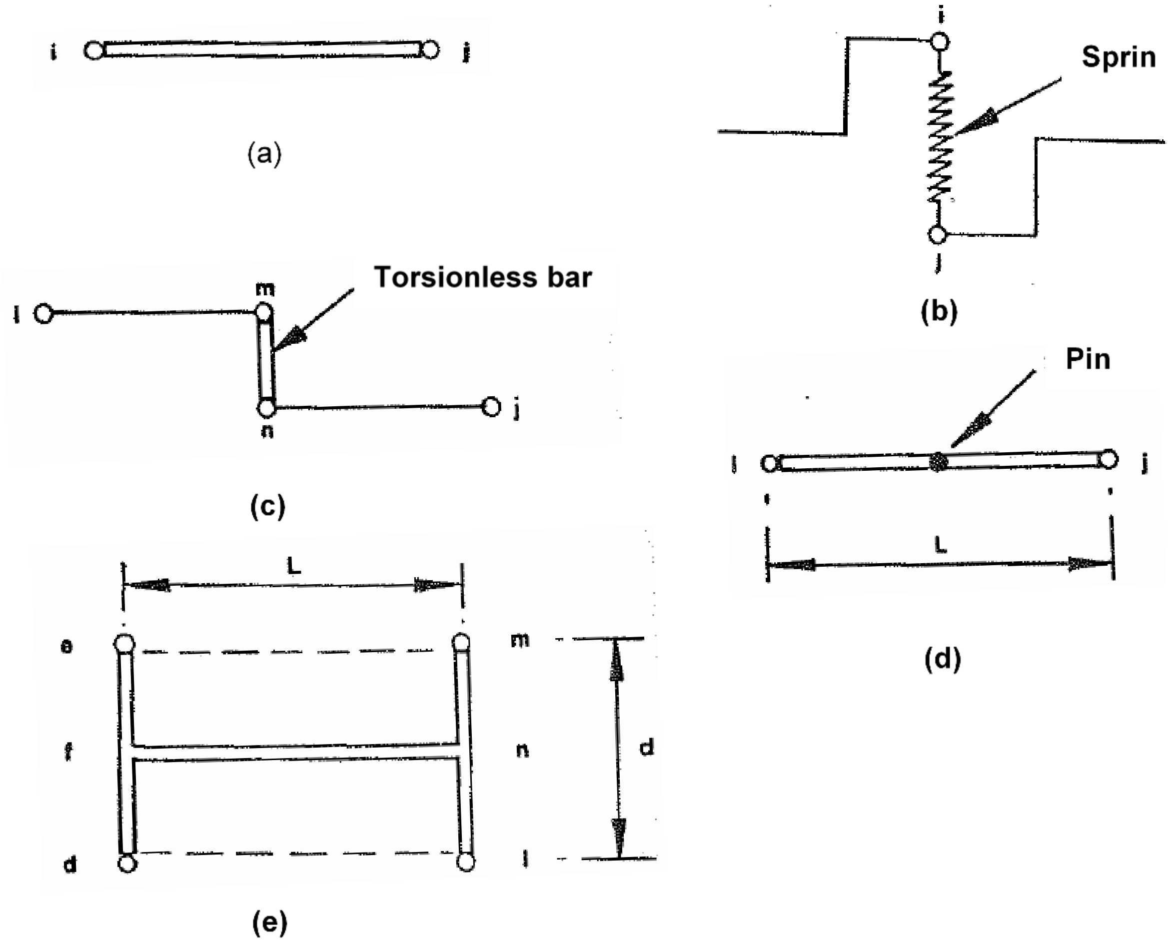

Source: Buckle (1984).

The transverse pre-compression force in the transverse tendons has no effect on the grillage model. This was based on the assumption that the force is sufficient to ensure that the longitudinal joints are an integral structural element of the bridge system. In other words, load transfer between adjacent beams is essentially preserved as long as satisfactory performance of grouted material is maintained and a sufficient level of pre-compression force is used.

Fu et al. (2011) conducted a study to investigate the behaviour of shear friction, which is used in the design of transverse post-tensioning in adjacent precast solid multi-beam bridges. Load testing was also conducted on a newly rehabilitated bridge to evaluate the effect of transverse post-tensioning under truck loads. Based on the study and test results, a numerical model was calibrated. The shear friction at the interface between adjacent beams depends on the interface characteristics and concrete type. The contact friction is specified by the coefficient of friction, which was taken as 0.6 for the interface between slab beams (see ACI 318-08 of American Concrete Institute 2008).

It is pointed out that the transverse post-tensioning improves the shear transfer strength of the interface between beams (Fu et al. 2011), even if the overlay and shear-key are cracked longitudinally. In this context, this shear transfer mechanism can be treated as shear friction. For a particular bridge, the level of transverse post-tensioning that ensures the whole bridge behaves monolithically could be found using finite element models (FEMs). In the FEM proposed by FU et al. (2011), which is based on ANSYS (Kohnke 1999) contact elements (e.g. see CONTA174 and TARGE170, in Kohnke 1999) are used to model the interface between longitudinal beams, while link elements are used to model the transverse post-tensioning rods (Figure 2.5). It was reported that the results from calibrated FEM matched the field test data.

Figure 2.5: Example of a 3D FEM

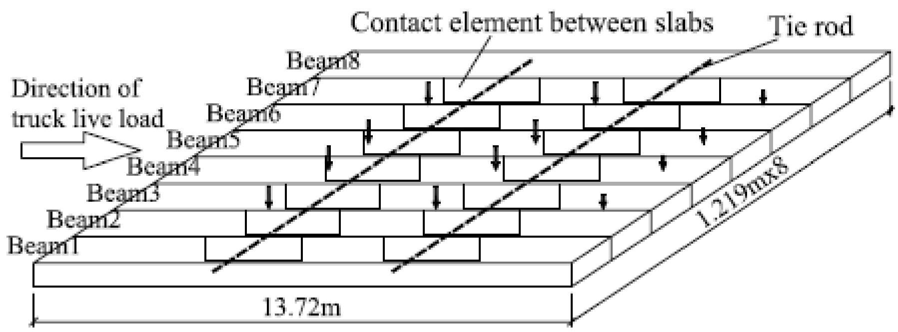

Source: Fu et al. (2011).

2.1.5 AASHTO Methods for Multi-beam Bridges

For multi-beam decks, the American Association of State Highway and Transportation Officials (AASHTO) method specifies a minimum pressure of 1.72 MPa on the face of the beams due to transverse stressing bars (AASHTO 2014). The bridge deck will then be considered to act monolithically as a unit. As a result, live load distribution factors for the beams can be obtained based on provided formulae. However, these formulae can only be applied for bridges with beams having approximately the same stiffness, thus they cannot be applied to TMR DU bridges with significantly stiffer upright KUs.

2.2 TMR Methodologies for Bridge Deck Analysis

TMR guidelines for the assessment of DU bridges have changed over time in order to incorporate information derived from in-house research. The typical methodologies are summarised below.

2.2.1 Bridge Analysis Models (BAM) for Heavy Load Assessment V1.0 (March 2011)

The sectional properties of members in the grillage models are defined as in West (1973), based on the following assumptions:

- The entire DU cross-section is used to model the longitudinal members.
- In the presence of diaphragms, the transverse members are modelled using the diaphragm height and web width equal to the transverse member spacing.
- The torsional constant for the longitudinal and transverse members is taken as 50% of the full torsional constant.
- All internal beams are modelled with reference to the uncracked properties
- Shear failure of individual units is not considered a valid failure mode and should not be considered.
- For cast-in situ kerbs, if modelled, the kerb properties are to be transformed using Equation 3.

$$b_{ef} = \frac{\sqrt{f_c' \text{ in situ}}}{\sqrt{f_c' \text{ precast}}}\, b \qquad (3)$$

where

b_{ef}	=	effective width of the transformed kerb section
b	=	actual width of the kerb section
f_c' in situ	=	yield strength of the in situ kerb concrete
f_c' precast	=	yield strength of the precast deck concrete

2.2.2 Design Assumptions for Standard DUs (Standard Drawing 1515)

The following assumptions have been made:

- Outer unit: the outer DUs for spans 10–25 m have been designed with a 40 MPa, 300 mm deep x 500 mm wide, cast in situ kerb. The kerb is transformed using Equation 4.
- Transverse stiffness for grillage model: transverse members have been modelled using section properties that are equivalent to 10% of the longitudinal member's section properties of 2 m spacing.
- Torsion stiffness: for ultimate cases, cracked sections were modelled using 20% of the section's uncracked torsion stiffness, torsion steel to be designed for cracked section analysis results only.
- Critical section:
  - internal members are modelled using full EI
  - external members are modelled using

$$I_{\text{kerb model}} = \frac{\frac{I}{y} \text{ outer unit}}{\frac{I}{y} \text{ internal unit}}\, I_{\text{internal unit}} \qquad (4)$$

  - the grillage model assumes equal centroid heights
  - the outer KU is not considered critical as it is constrained to the internal member by the transverse stress, meaning the strain in the bottom of the external and first internal DU will be nominally equal. The first internal member is considered the critical design member
  - the ultimate design load is considered to be the load which produces the first yield in the critical member.

The above method has been applied by consultants for the structural assessment of DU bridges on Flinders Highway. Results show that some structural members of three bridges (Canal Creek, HR Mayston and Namoi) are overloaded.

2.2.3 Technical Note S02: Modelling DU Bridge Superstructure for Tier 1 Assessment, v3.10 (TMR 2013)

Two modelling approaches have been used in assessment and design of DU bridges:

- approximate the distribution of loads at the serviceability limit state and the redistribution of the loads away from overloaded members such as kerbs and transverse members
- approximate the distribution of load at the ultimate limit state.

The recommended model approximates the distribution of load at the ultimate limit state based on the following assumptions:

- linear elastic grillage/frame models
- a single longitudinal member per DU or KU
- transverse members are orthogonal to the longitudinal joint between the DUs (not necessary for small skews – say less than 15 degrees)
- the bending stiffness of internal longitudinal members is to be calculated based on the uncracked properties of a typical internal DU
- the bending stiffness of the external longitudinal kerb members is to be determined such that the KU and the adjacent DU reach their ultimate bending strength having the same curvature. This is achieved by calculating the stiffness of the KU based on the ultimate bending moments of KU $M_{u.ku}$, and DU $M_{u.du}$, and the stiffness of the DU I_{du} by the following formula (Equation 5):

$$I_{\mathrm{ku}} = \frac{M_{\mathrm{u.ku}}}{M_{\mathrm{u.du}}} I_{\mathrm{du}} \tag{5}$$

  i.e. the KU will attract less moment, thereby resulting in a lower calculated bending moment in the KU.

- the transverse stiffness in bending is significantly lower than in the longitudinal direction, e.g. 3% of the longitudinal stiffness on a per metre basis
- the torsion stiffness of longitudinal members is 20% of the uncracked properties, i.e. the DUs are assumed to be cracked at the ultimate limit state
- zero torsion stiffness for transverse members.

While this modelling approach shows a consistency with the strength of the transverse members at the ultimate limit state without the need for load distribution, there is a dearth of work in field testing of the actual bridge under serviceability and ultimate limit state loads to validate the model.

2.3 Recommended Modelling Approaches

The following modelling methodologies are proposed for further calibration and validation:

- TMR approach (Technical Note S02)
- the Hambly (1991) method for DU bridges without shear-keys , where
  - pin joints are used to connect transverse elements, at locations that match of the mortar joints between the longitudinal elements that represent the DUs
  - full cross-sectional properties are used to define the longitudinal and transverse elements
  - the torsional constant of the longitudinal elements is taken as 20% of that defined for the full uncracked section

- the torsional constant of the transverse members is calculated based on the transverse stiffness of concrete only, and is taken as $D^3/6$ per unit length, where D is the thickness of the precast concrete beam, as used by Badwan and Liang (2007)
- no local adjustment of the KU stiffness is required.

3 IN-SERVICE MONITORING AND LOAD TESTING OF CANAL CREEK BRIDGE

3.1 Objectives

The objectives of the testing program were to:

- understand the structural behaviour of the test bridge under known loads, specifically
  - deflection profile of the bridge under a known load
  - relative load sharing between the deck and kerb units
  - the transverse behaviour of the bridge (behaviour of the contact surfaces between the deck units, degree of unit separation or rotation under service load)
  - dynamic response of the superstructure to the specific test vehicles
  - dynamic response of the headstocks at the pier and abutment to the specific test vehicles.
- review the influence that different test vehicles have on the dynamic response of the test bridge
- review the in-service performance of the test bridge under ambient traffic, in particular
  - peak strains, deflections and other measurements under in-service loading
  - improved understanding of in-service traffic (and movements)
  - identification of any specific loading risks.
- provide data to calibrate analytical assessment models for transverse deck unit bridges of a similar era (up to the service limit state).

3.2 Canal Creek Bridge

TMR Bridge N. 7703 (Figure 3.1), over Canal Creek, is a two-span simply-supported structure, with DU superstructure at chainage 93.845 km on Flinders Highway, approximately 40 km east of Cloncurry, Queensland. Each span is 8.33 m long and 7.32 m wide, with 6.70 m between kerbs. The bridge is located on a heavy vehicle or higher mass limit (HML) route (TMR ID: RT2). The HML RT2 route is crossed by up to 400 vehicles per day, with 30% of the traffic consisting of heavy vehicles.

Bridge N. 7703 was designed in 1969 for H20-S16 class vehicle loading and is representative of a DU bridge type mostly designed according to pre-1969 standards. TMR has identified this DU bridge type as representative of at-risk structures. The bridge construction was completed in 1970.

Figure 3.1: View of Bridge N. 7703 over Canal Creek

Source: TMR.

3.3 Site Testing Program

The site testing exercise was undertaken between 29 April and 6 May 2014. The instrumentation plan included 56 sensors, mostly placed on the deck soffit in the midspan location.

The load tests consisted of nearly-static vehicle runs, with both single vehicles and a vehicle group crossing the bridge for each test. The vehicle group had an identical vehicle line-up for each run, with a crane at the front followed by a steel-suspension semi-trailer and an air-suspension semi-trailer. After the static load tests, vehicles runs at different speeds were conducted both for single vehicles and the vehicle group. All runs were replicated in both directions of traffic.

3.4 Results

3.4.1 Static Response

The measured response of the deck under static load tests was compared with estimates from a grillage model developed in accordance with the TMR guideline (Section 2.2), in terms of both tensile strains and deflections.

In detail, using the 48 t crane as the test vehicle, the measured tensile strains are mostly lower than estimated, with a percentage difference of 10–30% depending on the vehicle position (Table 3.1). On the other hand, the estimated deflections largely deviate from the measurements, with values from the grillage model up to 10 times greater than the measurements.

Despite the inevitable errors intrinsic to instrumental measurements and long recordings with high sampling rates, the estimated strains approximately matched the estimated values. On the other hand, the large deviations of the estimated deflections flag the failure of the TMR modelling methods in predicting the actual bridge behaviour.

Table 3.1: Deck response under 48 t crane: static test results vs DU theoretical estimates

	Vehicle path					
	Movement along the deck centreline			Tyre edge positioned at 0.3 m from the kerb		
Parameter	Measured ($\mu\varepsilon$)	Estimated ($\mu\varepsilon$)	Percent change	Measured (mm)	Estimated (mm)	Percent change
Maximum tensile strain	67	89	31%	93	104	12%
Maximum deflection	1.5	16.2	1000%	2.6	16.2	600%

3.4.2 Load Distribution

The load distribution factor (LDF) for each unit, as derived from the strain measurements, is shown in Figure 3.2 and Figure 3.3, for static vehicles and vehicles travelling at different speeds. The reference vehicle used for all sets of tests is the 48 t crane. With reference to the crane positioned within one of the two traffic lanes, the maximum LDF is 12.8% and the minimum is 5%. With the vehicle travelling within each lane at different speeds, the LDF appears to decrease with increasing speed. The overall maximum is essentially unchanged from nearly-static speeds up to 40 km/h (12.8%), while for higher speeds the LDF appears to decrease by 25% (Figure 3.2).

Figure 3.2: Maximum LDF under static loads

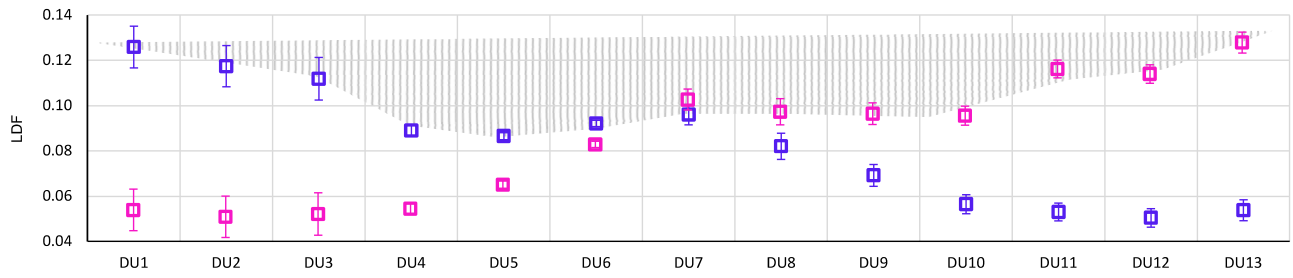

Note: Maximum LDF values related to vehicle tests performed on the lane carrying the traffic towards Cloncurry (purple squares), and to vehicle tests performed on the lane carrying the traffic towards Julia Creek (magenta squares), as derived for each DU. The envelope of the maximum LDF for each DU, from all static tests combined, is shaded in grey. The error bars indicate the standard deviation of the data from each set of tests.

Figure 3.3: Maximum LDF vs speed

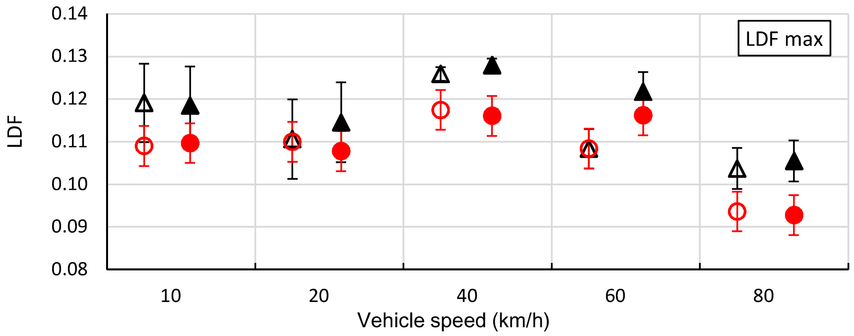

Note: Maximum LDF values derived for vehicle runs at different speeds. The vehicle used for the tests is a 48 t crane. The red circles indicate the LDFs derived for the inner DUs, while the black triangles are the LDF values derived for the KUs. Hollow markers refer to tests performed on the lane carrying the traffic towards Cloncurry, while solid markers indicate values obtained from tests performed on the lane carrying the traffic towards Julia Creek. The error bars indicate the standard deviation of the data from each set of tests.

3.4.3 Dynamic Response

Consistent with the bridge span length and width, the first fundamental frequency was measured at 12.3 Hz and associated with bending in the longitudinal direction, while the second fundamental frequency was 14.6 Hz and associated with bending in the transverse direction. With a near-unity span/width ratio (1.1), the fact that both the first and second mode shapes correspond to the sagging moment curvature, in the transverse and longitudinal directions, confirms that the deck response is governed by bi-axial moments. It is noted that such a dynamic behaviour is common for short-span flat-slab reinforced concrete superstructures.

3.4.4 Short-term Monitoring

The maximum tensile strain measured under ongoing traffic was 98 $\mu\varepsilon$, i.e. 5% greater than the 93 $\mu\varepsilon$ measured under static tests (Table 3.1). It is noted that the 5% difference in the maximum strain measurements is within the minimum error intrinsic to the sensor and data acquisition systems, especially over long recordings. Over each 24-hr cycle, no more than one event was recorded at the maximum tensile level.

3.4.5 Deflections and Relative Movements

The maximum deflections measured under static tests reach 3.3 mm, under the passage of the 48 t crane. The measurements are consistent with the vehicle crossing the bridge in both directions of traffic. The crane also induced the maximum relative displacements between adjacent units, with a relative gap reaching 0.14 mm near the tyre footprint.

3.4.6 Investigations into Dynamic Load Amplification

No conclusive results in terms of dynamic load amplification can be derived from the tensile strain measurements from all tests combined, i.e. short-term monitoring, static tests, and vehicle runs at controlled speeds.

In detail, the measured strains appear to undergo different changes for tests carried out in the two directions of traffic. With reference to the 48 t crane, for the static tests and the runs at different speeds, the maximum measured tensile strains vary by ±10%, with strains increasing by 10% when the vehicle crossed the bridge at 80 km/h towards the Cloncurry direction, and decreasing by the same amount when the vehicle travelled at the same speed in the opposite direction. The increment of the load amplification induced by the different test vehicles (i.e. crane, semi-trailers and road train) also appears to be inconsistent in the two directions of traffic (Figure 3.4 – Figure 3.6). As noted in Section 3.4.4, the maximum strain measured under ongoing traffic is 5% greater than the maximum strain measured during static tests.

Figure 3.4: Strain increment vs vehicle speed (crane)

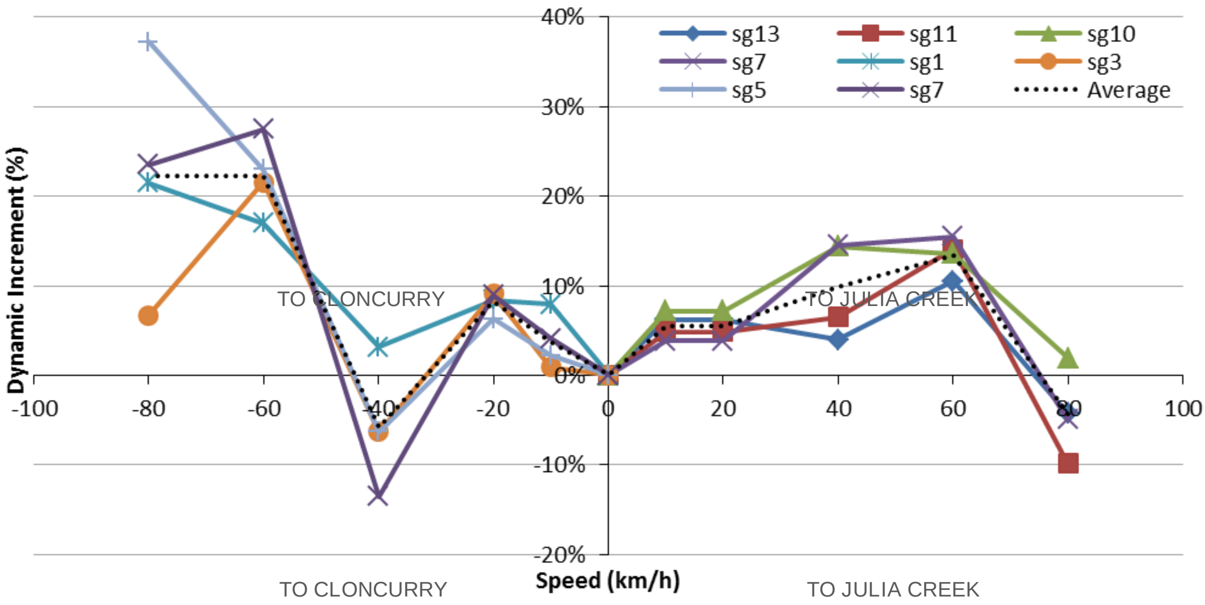

Note: Maximum strain increment measured with respect to the static strains under the passage of the 48 t crane.

Source: Ngo and Pape (2015), Figure 5.56.

Figure 3.5: Strain increment vs vehicle speed (semi-trailer 2)

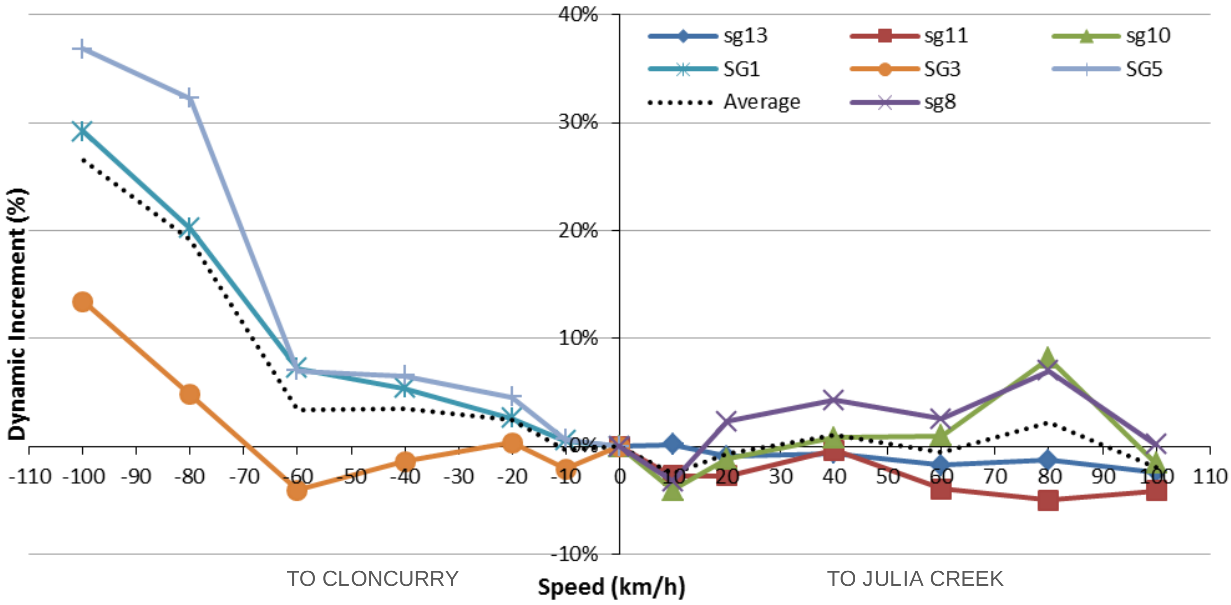

Note: Maximum strain increment measured with respect to the static strains under the passage of the 'semi-trailer 2' vehicle.
Source: Ngo and Pape (2015), Figure 5.58.

Figure 3.6: Strain increment vs vehicle speed (all test vehicles)

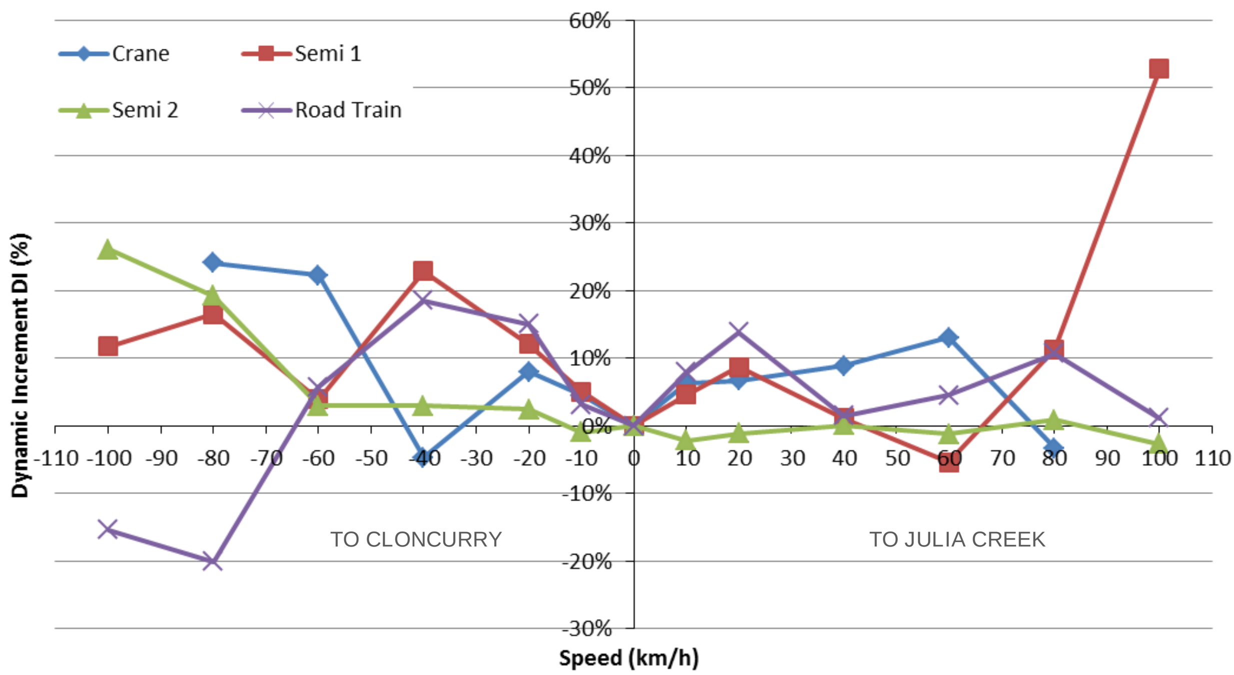

Note: Maximum strain increment measured with respect to the static strains under the passage of all test vehicles.
Source: Ngo and Pape (2015), Figure 5.55.

4 LABORATORY TESTING OF INDIVIDUAL DECK AND KERB UNITS

4.1 Objectives

The objectives of the testing program on individual beams were as follows:

- measure the properties of each DU and KU, specifically in terms of
  - vertical stiffness and thus, inertia, and variation with increasing deflections
  - bending and shear capacity at ultimate limits
  - cracking patterns and evolution up to failure
  - failure mechanism
- measure the materials properties from
  - concrete cores
  - reinforcement cores
  - assessment of prestress losses.

4.2 Deck and Kerb Unit Samples

A sample of four 9.1-m long DUs, two DUs and two KUs, salvaged from decommissioned bridges were used for the testing program.

Although the source bridges could not be identified, based on the unit size and prestressed reinforcement, the salvaged KUs were consistent with TMR standard drawings, as shown in Figure 4.1 (detail *'a'*). For the two DUs, while unit dimensions as well as the properties of the prestressed cables could be matched by the standard drawings, the cable arrangement is slightly different (detail *'b'* in Figure 4.1). A summary of the cross-section and material properties detailed in the relevant standard drawings is given in Table 4.1.

Figure 4.1: DU cross-section

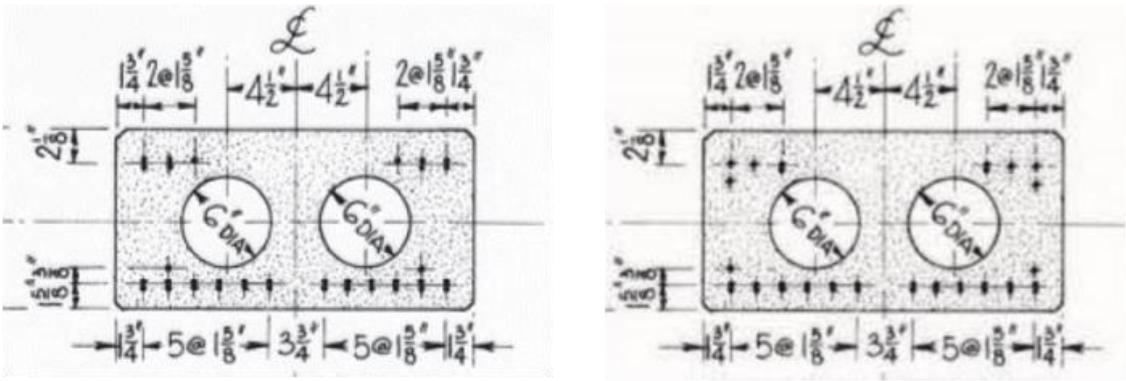

(a) Standard drawing (b) Actual deck unit used

Note: Comparison between standard DU details as from as-built plans of similar bridges (a), and the section that matches the DUs used for the laboratory testing (b) (as from TMR drawings S803 and S906).

Source: Ngo et al. (2016), Figure 2.1.

Table 4.1: Summary of test unit properties

Items[1]	Deck units (DU)	Kerb units (KU)
Design era	1963	1963
Length (mm)	9093	9093
Height of cross-section (mm)	305	673
Width of cross-section (mm)	597	305
Void/solid	2 x 152 mm dia. voids	Solid
Number of transverse stressing points	4	4
Minimum concrete strength at transfer (MPa)	31	27.6
Minimum concrete strength at 28 days (MPa)	41.4	34.5
Density of concrete (kg/m^3)	2550	2550
Elastic modulus of concrete (MPa)	35 627	32 523
Prestressed reinforcement	36/7.0 mm dia. high tensile straight wires	19/7.0 mm dia. high tensile straight wires
Area of wire (mm^2)	38.6	38.6
Initial strand force (kN)	45.1	45.1
Yield strength (MPa)	1620	1620
Elastic modulus (MPa)	137 700	137 700

Note 1 -- The specimens tested in shear are DU-S and KU-S, and in bending are DU-B and KU-B.

Source: Ngo et al. (2016), Table 4.1.

All beams exhibited damage to a varying extent. The pre-existing damage was due to the deteriorated original superstructure as well as the salvaging process, and was likely aggravated during transport to the laboratory. Cracks in the concrete up to 2.5 mm width were present in the KUs, and moderate-to-severe concrete spalling was present in three units. One of the DUs (DU-2) was in overall good condition, with minor cracking and isolated concrete spalling.

4.3 Laboratory Testing Program

The laboratory tests were undertaken at the Structures Laboratory at the University of Queensland between 23 June and 3 July 2015. The instrumentation included load cells in-built into the testing frame, and string potentiometers placed at the midspan and quarterspan sections to measure the beam deflections (Figure 4.2).

The load tests consisted of incremental load cycles, with load points designed to assess both the shear and bending behaviour of the beams. In detail, the bending tests were carried out with four load points, i.e. by placing the load in two transverse locations separated by a distance of 2250 mm, or 1125 mm on each side of the midspan section. The shear tests were performed by placing two load points, with the load placed in one transverse location at a distance of 1260 mm from the closest support position. The support location was adjusted for each test to maximise the effects of the applied bending or shear forces.

One KU and one DU were tested to ultimate bending, and the remaining two units were tested in shear.

Figure 4.2: Testing arrangement – view of the testing frame set-up for shear load testing of a DU (DU-1)

Source: Ngo et al. (2016), Figure 2.3.

4.4 Results

All bending and shear testing measurements are summarised in Table 4.2. Detailed comments are provided below.

Table 4.2: Summary of test results

Test[1]	DU-S	KU-S	DU-B	KU-B
At elastic limit				
Applied load (kN)	200	240	110	115
Maximum shear (kN)	171	208	–	–
Maximum bending moment (kNm)	– [2]	–	172	180
At fracture				
Applied load (kN)	320	520	150	220
Maximum shear (kN)	269	451	–	–
Maximum bending moment (kNm)	–	–	242	344
At ultimate limit				
Ultimate applied load (kN)	397	625	235	280
Ultimate shear capacity (kN)	331	542	–	–
Ultimate bending capacity (kNm)	–	–	372	439
Estimated ultimate shear capacity (kN)	189 (204) [3]	314 (334)	–	–
Estimated ultimate bending capacity (kNm)	–	–	317 (365)	430 (455)
Actual to theoretical ratio	1.75 (1.62)	1.73 (1.62)	1.17 (1.02)	1.02 (0.96)
Location of failure	Under actuator, 30^0 diagonal crack toward support	Under actuator, 60^o diagonal crack through a hole	Under actuator P2, diagonal crack, explosive	Close to midspan, vertical crack, little warning
Failure mode	Shear compression failure, explosive	Diagonal tension failure	Flexural-shear failure	Pure bending
Maximum midspan deflection (mm)	93.6	32.9	273	69
Curvature at failure (m^{-1})	–	–	0.0365	0.0182

Note 1 – The specimens tested in shear are DU-S and KU-S, and in bending are DU-B and KU-B (Ngo et al. 2016, Table 4.1).

Note 2 – The missing values are either not applicable or not evaluated.

Note 3 – Numbers in parentheses () are revised estimates based on the measured material properties.

4.4.1 Performance in Bending

The observed bending capacity of the test units correlated well with theoretical predictions.

In particular, the DU showed a highly ductile failure, with large deflections and curvature before failure (Figure 4.3). The ultimate failure with extensive cracking throughout occurred suddenly.

As expected, the KU exhibited much higher stiffness under the vertically applied load, with a significantly smaller bending curvature than that derived from the DU test (Figure 4.4). Significant cracking appeared in the KU loaded with 115 kN, when the midspan deflection reached 7 mm. Thus, the KU performance beyond the elastic range was characterised by a limited ductility, especially if compared with the behaviour of the DU under similar loads (Figure 4.5).

4.4.2 Performance in Shear

The observed shear capacities of both DU and KU exceeded theoretical predictions. Despite the fact that the units used for the shear tests were in poor initial condition, the shear capacity appeared to be slightly affected by the pre-existing damage (Figure 4.5 and Figure 4.6). The testing results imply that the theoretical assumptions and assessment methods used to estimate the beam shear capacities are conservative.

Both the kerb and DU displayed a brittle failure in shear, with significant shear cracking in the DU at 7 mm deflections (Figure 4.5), and across the KU at 4 mm deflections (Figure 4.6). A structural failure in this deflection range points to inadequate shear reinforcement of the tested specimens.

Figure 4.3: DU load-deflection curve in bending

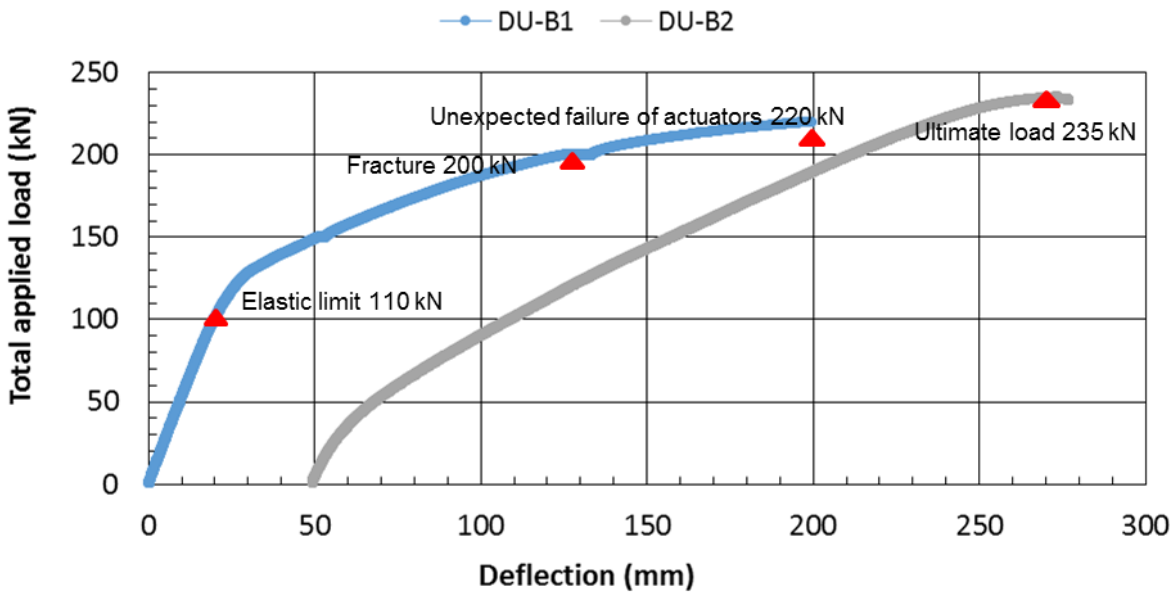

Note: Load curve derived for the testing in bending of the DU. The test was carried out in two cycles, i.e. up to an external force of 220 KN (DU-B1), followed by unloading and reloading to failure (DU-B2).

Source: Ngo et al. (2016), Figure 4.18.

Figure 4.4: KU load-deflection curve in bending

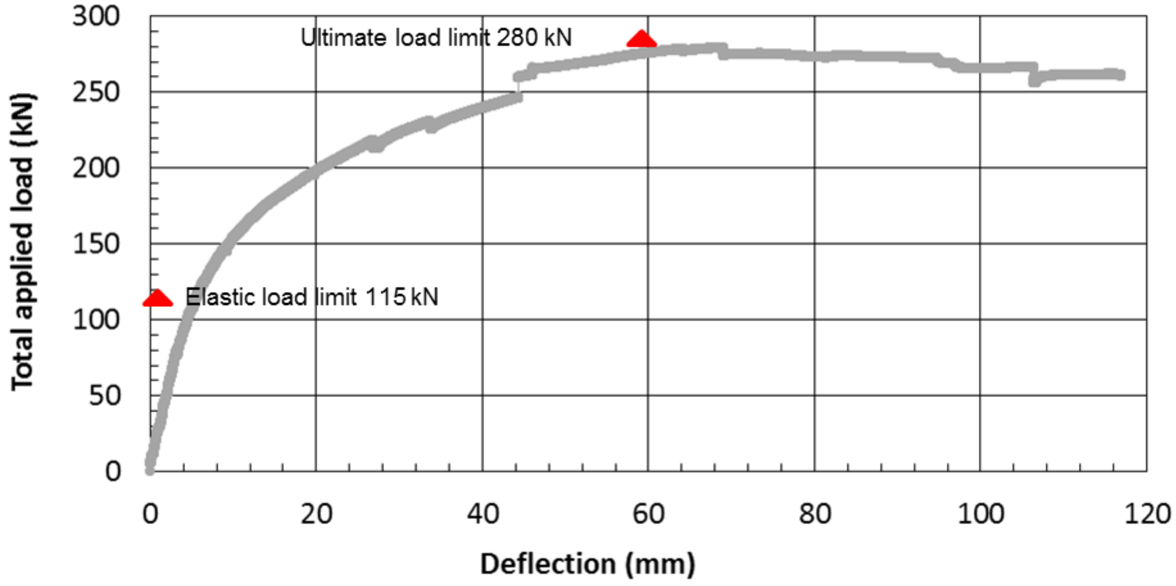

Note: Load curve derived for the testing in bending of the KU. The test was carried out in a single stage, up to a maximum external load of 280 kN.
Source: Ngo et al. (2016), Figure 4.24.

Figure 4.5: DU load-deflection curve in shear

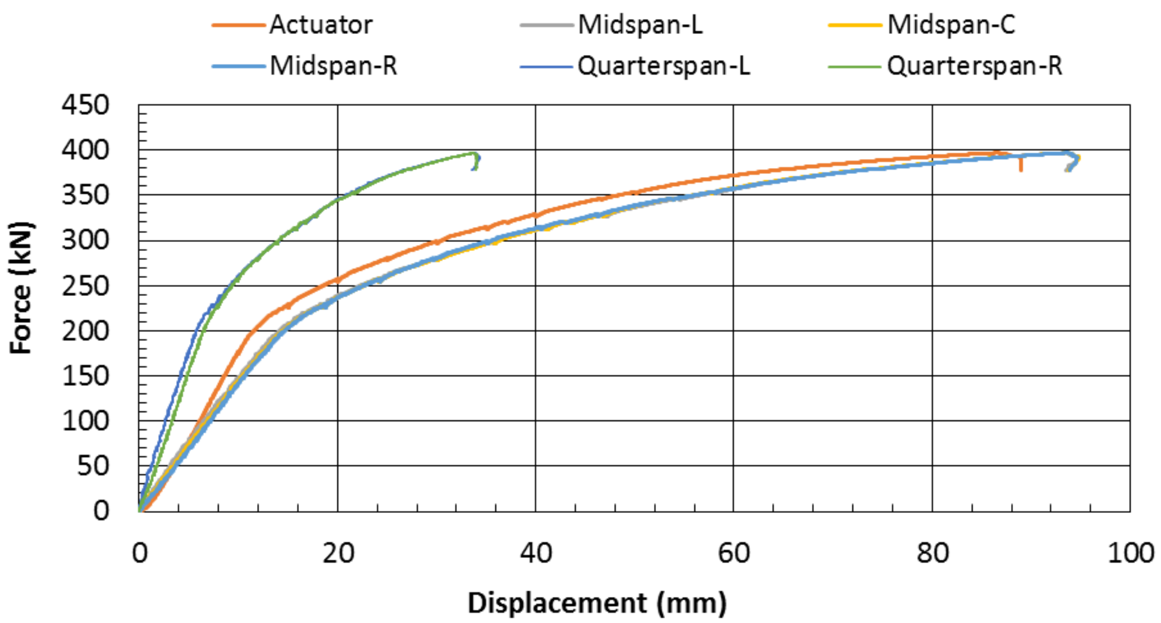

Note: Load curve derived for the testing in shear of the DU. The test results were recorded in three transverse locations in midspan (L – left, C – centre, and R – right), and in two transverse locations in quarterspan (L – left, R – right).
Source: (Ngo et al. (2016), Figure 4.9.

Figure 4.6: KU load-deflection curve in shear

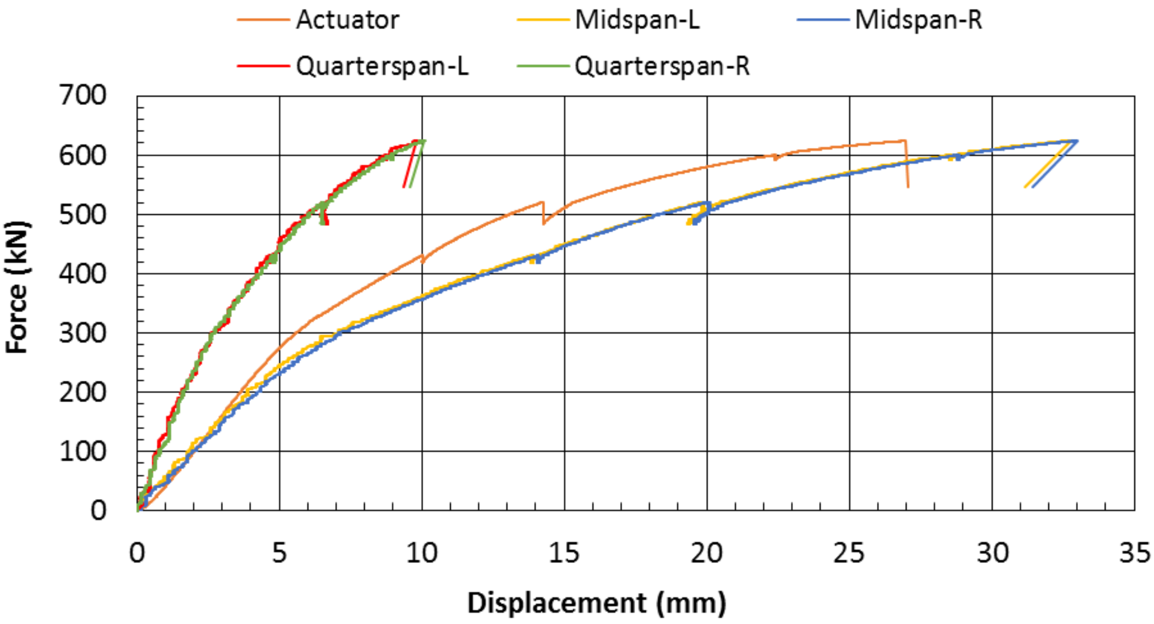

Note: Load curve derived for the testing in shear of the KU. The test results were recorded in three transverse locations in midspan (L – left, C – centre, and R – right), and in two transverse locations in quarterspan (L – left, R – right).

Source: Ngo et al. (2016), Figure 4.1.

4.4.3 Material Properties

The material tests carried out on concrete cores from all unit specimens yielded a characteristic cylindrical strength of 65 MPa for the DUs and 60 MPa for the KUs. Such values are significantly higher than what were assumed for the assessment of DU bridges.

The prestressed cable strength f'_p = 1620 MPa matched the design specifications.

It is worth noting that the measured strengths were derived from a limited number of samples, therefore, they may not be representative. Further testing would be recommended to validate the actual material strengths.

4.4.4 Other Considerations

The following are worth noting:

- The results obtained from this testing campaign are relevant for DU bridges of span length equal or similar to that of the tested units.
- While the tests showed that both DU and KU have higher than estimated capacities and a more ductile behaviour at failure than expected, a DU bridge deck might display a less ductile behaviour prior to failure.

5 LABORATORY TESTING OF A PARTIAL DU BRIDGE

5.1 Objectives

The objectives of the testing program on a partial DU bridge were to measure the response of the integral deck up to failure, specifically in terms of:

- load transfer and distribution factor
- load re-distribution prior to failure
- ultimate load capacity of joined KUs and DUs
- joint behaviour near failure and maximum deflections
- controlling failure mechanism.

5.2 Characteristics of the Partial DU Bridge

5.2.1 *Construction Limitations*

The test structure was built in light of the following constraints:

- The structure's construction was carried out in accordance with the fabrication specifications for DU bridges, as for the standard drawings provided by TMR.
- Based on the available beams, the test structure was built to reproduce half a deck, with a single simply-supported span of 7.86 m length between the supports, and overall width of 4.0 m, approximately corresponding to half of the width of an ordinary DU bridge.
- The real-life superstructure supports were reproduced via elastomeric bearings placed on top of steel strong-backs.
- The test structure consisted of six 8.3-m long DUs and one KU, tied transversely by four 29 mm diameter TSBs. All units, as salvaged from decommissioned bridges (details in Figure 5.3), had a skew of 10 degrees.
- Due to permanent deformations, some of the units exhibited a pre-existing bending curvature.
- The gaps between the units were filled by a 25 mm layer of mortar.
- After the mortar had cured, the TSBs were tensioned and grout was injected in the TSB ducts, in accordance with the original fabrication specification.
- Regular grade bars were used for the TSBs, with a prestress force P = 175 kN on each bar. The applied P value corresponds to 50% of the design prestressing force, so as to reflect possible prestress losses or other deterioration usually associated with TSBs in aging DU bridges.

5.2.2 *TSB Installation*

To remove each unit from the bridges, the original TSBs were cut and left in place. Therefore, new TSB ducts had to be drilled through the units in the partial DU bridge. In detail, to allow the deck to be assembled, 50 mm diameter ducts were drilled across the width of each unit in four locations, at 2185 mm spacing. The resultant layout of the test structure is shown in Figure 5.2, while the plan view is reproduced in Figure 5.3.

It is noted that, due to the fact that the salvaged unit had a minor skew, while coring through the concrete had to be carried out with caution to avoid cracking, the resultant TSB ducts were slightly misaligned between adjacent units.

Figure 5.1: KU and DU cross-sections

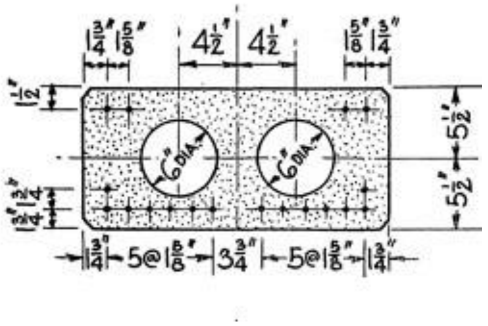

Note: 1 inch = 25.4 mm

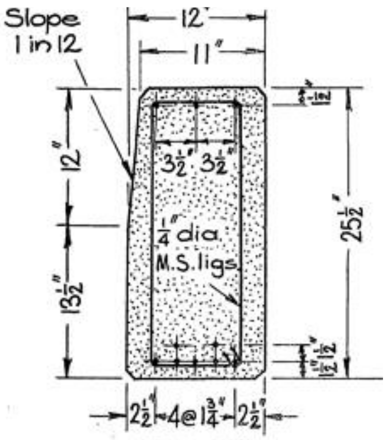

(a) DU

(b) KU

Note: Details of the six DUs used for the partial DU bridge (a) and of the single KU (b).
Source: Ngo (2017), Figure 2.1.

Figure 5.2: Sections of the test structure

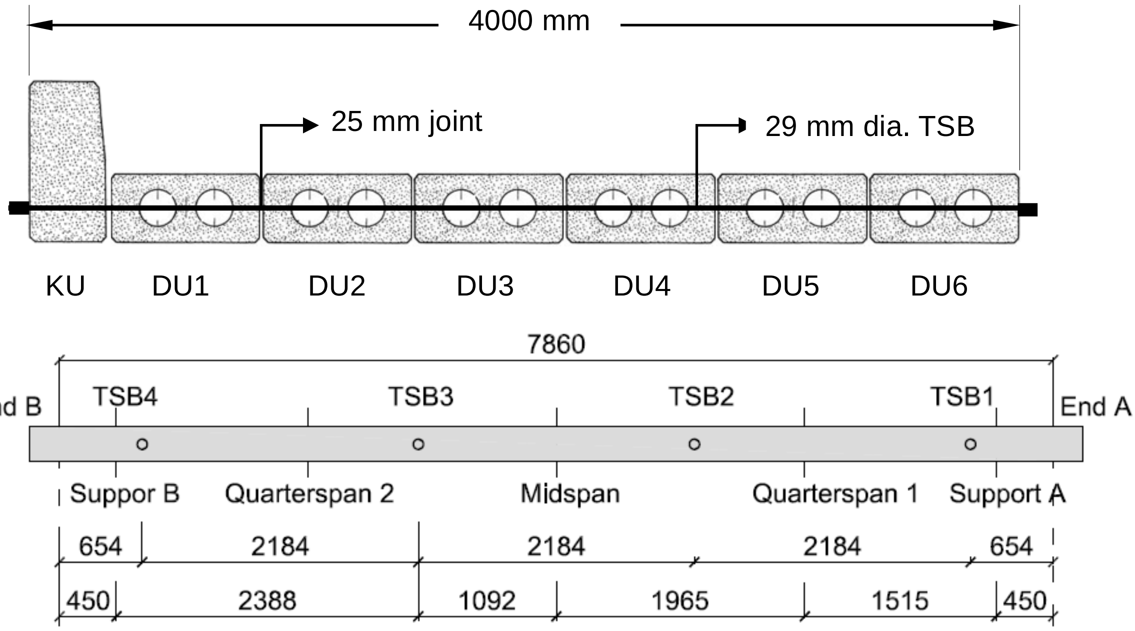

Note: Cross-section of the test structure in the transverse direction (top) and in the longitudinal direction (bottom).
Source: Ngo (2017), Figures 2.5 and 2.6.

Figure 5.3: Loading configurations

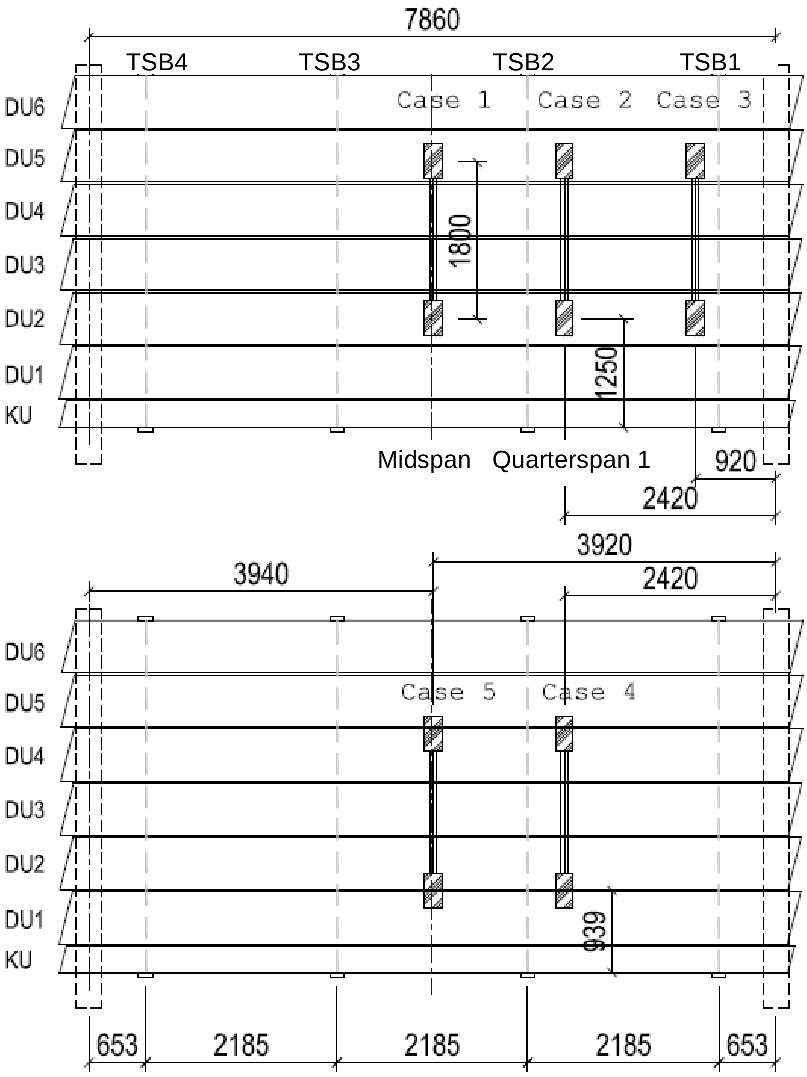

Note: Plan view of the test structures with details of the load configurations, which reproduce the load patches associated with a heavy vehicle's axle. Load cases 4 and 5 were placed closer to the KU (bottom).

Source: Ngo (2017), Figure 3.2.

5.3 Laboratory Testing Program

The laboratory tests were undertaken at the Structures Laboratory at the University of Queensland between 28th July and 6 October 2016. The structure was instrumented with a system of 106 sensors, installed in midspan, quarterspan, near the supports, and along two TSBs. Beside the load cells, the instrumentation included:

- 26 strain gauges placed at the top and bottom concrete surfaces of each unit
- 14 strain gauges on the side of the unit, at about mid-height
- 29 string potentiometers to measure deflections from the soffit of each unit
- 6 strain gauges on the TSBs
- 10 proximity probes at the joints between adjacent units to measure gap opening, placed both on the top and bottom of the deck

- 4 tilt meters at mid-width of every second unit to capture the transverse curvature of the deck under increasing load
- 6 tilt meters at mid-width of each unit in midspan to measure the variation of the longitudinal curvature under increasing load
- 11 strain gauges on the longitudinal prestressing cables installed after the completion of the tests under serviceability loads.

The load tests consisted of cycles of incremental load, with load points positioned in accordance with five defined load cases (Figure 5.3).

The tests under serviceability loads were repeated for up to three cycles, while only one load cycle was necessary to reach the ultimate state limits.

5.4 Results

Before discussing the findings from this testing program, the following points should be noted:

- Due to the lack of restraints along DU6 to simulate the presence of the other half of the deck, the performance measured for DU6 and, by close association, also for DU5, likely deviates from that of an inner DU close to the deck centreline. Therefore, the test results derived for DU1–4 are discussed in the report.
- Due to the inherent difficulties of building a full-scale bridge deck in the laboratory, it is likely that the TSBs were not connecting the units to the same extent as real-life DU bridges.
- The supports reproduced in the laboratory likely did not replicate the exact support properties and conditions of aging DU bridges.

5.4.1 Performance up to Failure

The tensile strains measured under serviceability loads in bending appear to be in the same range as those measured for the Canal Creek Bridge, which has a similar span length (Section 3). In particular, the measurements obtained from the site testing of the Canal Creek Bridge under the passage of the 48 t crane, positioned next to the kerb, are comparable to the results from the bending tests under equivalent axle load and configuration (Table 5.1).

Table 5.1: Test bridge vs Canal Creek Bridge – comparison of tensile strains and deflections

	KU		**DU**	
Measurement in midspan	Canal Creek Bridge	Test bridge(1,2)	Canal Creek Bridge	Test bridge (1,2)
Tensile strain (με)	96	65	93	86
Deflection (mm)	2.6	1.8	2.7	2.5

Note 1 – The maximum is taken between the DU1–4 measurements.

Note 2 – The load configuration is for load case 5, and values correspond to an applied load of 120 kN.

As listed in Table 5.1, the comparison seems to highlight the fact that the KU in the test bridge has a slightly stiffer behaviour than that derived from the site measurements. On the other hand, it should be noted that the two sets of measurements are affected by different types of error. Errors in the laboratory measurements are by default smaller, although the test structure does not exactly reproduce a real-life bridge deck.

The overall performance of the test bridge exceeded expectations. With reference to the load-deflection curve shown in Figure 5.4, which is based on the measurements taken in midspan, the test structure failed in bending at 1040 kN with the KU cracking first followed by failure of the DUs.

The structure's elastic behaviour was measured up to 250 kN (25.1 t), which yields DU tensile and compressive strains of 170 $\mu\varepsilon$. The elastic limit corresponds to a maximum deflection of 4.8 mm, as measured for DU1–4.

Figure 5.4: Load-deflection curves in bending, derived for all units up to failure

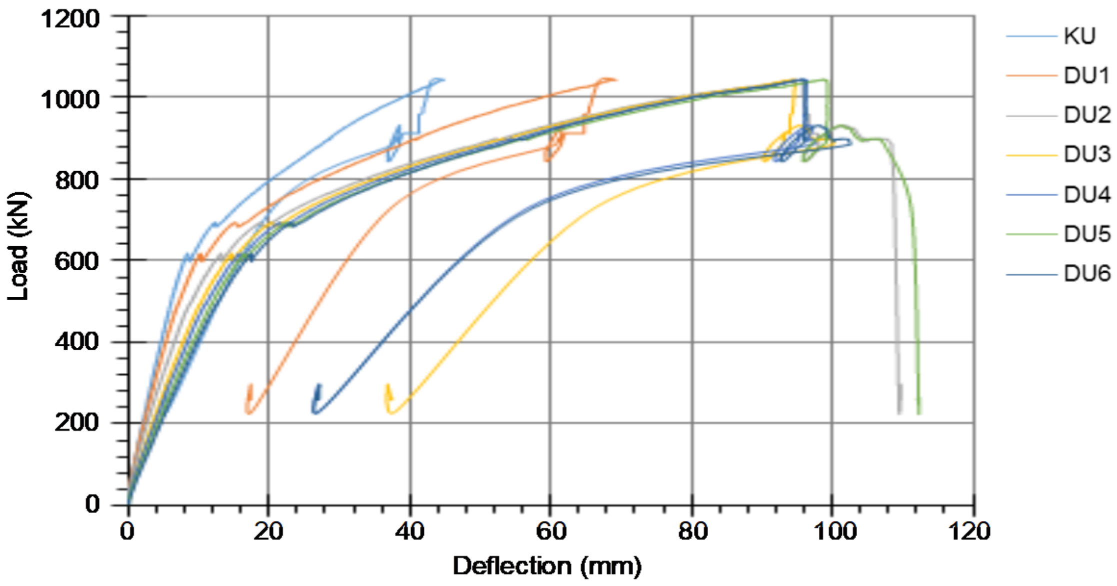

Source: Adapted from Ngo (2017), Figure 5.17a.

5.4.2 Load Distribution

Despite the highly ductile failure mode (Figure 5.4), at high load levels marginal load re-distribution was observed between the KU and the DUs, which is an indication of negligible contribution of the TSBs to the performance of the whole structure.

Specifically, the LDF varies between the DUs from 7.8% (DU1) and 14.2% (DU6), increasing or decreasing by 1.0±0.5% from the first to the last load increment (Figure 5.5). For the KU, the LDF is three times greater than that associated with the DUs, reaching a maximum of 39%. However, the KU LDF variation between tests is more significant and up to 20%, and does not seem to have a correlation with the external load.

The average LDF for DU1–4 is 10.3%. All DUs do not exceed an LDF of 12% prior to failure.

Figure 5.5: LDF vs load for all units derived for each 125 kN increment of the applied load

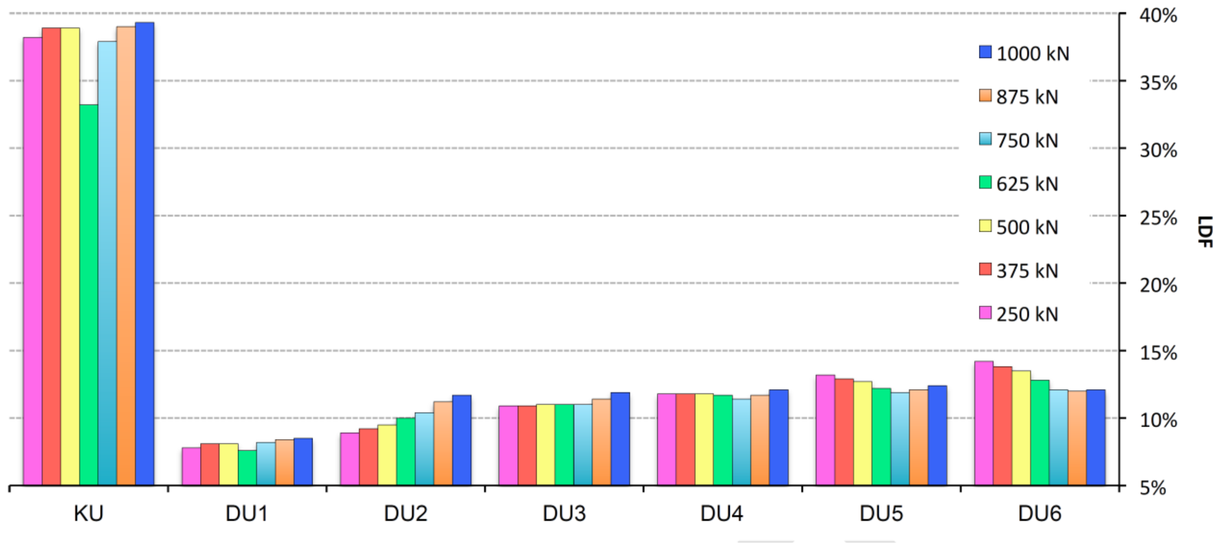

5.4.3 Joint Movements

The relative movements of adjacent units appeared to depend on the position of the unit with respect to the position of the loading points. At failure, the gap at the joint opened up to 4 mm, with the largest opening measured between DU1 and DU2.

The elastic limit was identified with a gap of 23 μm, opening on the deck soffit between DU4 and DU5. Transverse rotations associated with the elastic response reached 20 millidegrees in DU5. The longitudinal curvature peaked at 50 millidegrees in midspan for DU4–5.

5.4.4 Material Properties

The derivation of the concrete properties was based on three concrete cores from the DUs and three cores from the KU. Given the lack of an adequate number of samples to derive averages and outliers, the error on the derived concrete properties cannot be estimated. In light of that, the concrete tests yielded a rather high f'_c = 53 – 64 MPa for the DUs, and f'_c = 69 MPa for the KU. These values are significantly greater than those assumed for the type of concrete used in DU bridges.

For the maximum tensile stresses measured in the prestressed cables, 1848 MPa was derived for the DUs and 1802 MPa for the KU. The average prestress loss was measured at 37% for the DUs and 40% for the KU, although dependent on the assumption of the initial prestress levels. All these values are higher than design specifications and what are normally assumed for theoretical estimates.

The steel reinforcement tests resulted in 460 MPa yield strength and ultimate strength measured at 548 MPa, which are also significantly higher than the design values (245 MPa).

6 LOAD TESTING OF SANDGATE ROAD BRIDGE

6.1 Objectives

The last component of the project was devised to investigate the role of the TSBs in the bridge deck performance and to quantify the impact of TSB deterioration. Therefore, measurements from an operational bridge were taken in two different scenarios:

- continuous monitoring of the bridge response under operational traffic (i.e. unknown travelling loads)
- load testing under known quasi-static loads, before and after the introduction of incremental TSB damage.

The main objective of the monitoring was to identify the benchmark behaviour of the structure. The main objective of the load testing was to investigate the changes in the behaviour of the DUs when damages in the TSBs were incrementally introduced, specifically in terms of:

- concrete strains and variation
- vertical deflections of the DUs
- movements of the mortar joints between the DUs
- load distribution between the DUs and related variation.

A Roads and Maritime Services (RMS) proof load vehicle was used for the controlled load testing.

6.2 Sandgate Road Bridge

TMR Bridge No. 8558, built in 1985–86, carries the two northbound lanes of the Gateway Motorway (M1) across Sandgate Rd in Boondall (Brisbane), with width between kerbs of 8.5 m. The structure consists of 10 simply-supported spans, with span length between 14 and 18 m. In each span, the deck is made of 15 rectangular precast hollow units, which are transversely post-tensioned by 29 mm diameter TSBs, spaced every 2 m, with an asphalt DWS of 80 mm thickness.

All spans have a skew of $\theta = 13°$. Except for pier 5, where the DUs are seated on elastomeric bearings, each DU is anchored to the piers via 30 to 36 mm diameter dowels (galvanised bolts) of 800 to 920 mm length – depending on the span length – which are grouted into sockets in both the DUs and the headstocks.

Given the simply-supported deck system and constraints due to the construction schedules, TMR made arrangements for carrying out the performance testing on a single span. Thus, the 16m long span 9 was instrumented for in-service monitoring and load testing (Figure 6.1).

At the time of the testing, 11 out of the 15 DUs in span 9 exhibited longitudinal cracking to varying extent, likely caused by alkali-silica reaction (ASR), and mostly localised within 2.8 m from the supports.

Figure 6.1: View of span 9 of Sandgate Rd Bridge

Notes: Span 9 is supported by pier 8 (left) and pier 9 (right).

6.3 Site Testing Program

The response of the deck in span 9, under ongoing traffic/ambient excitation, was recorded from 28 February to 8 March 2017. The load tests in span 9, performed before and after incremental TSB severing, were carried out from 9 to 13 March. The TSB severing process is shown in Figure 6.2.

As in the simplified schematic shown in Figure 6.3, the instrumentation included 87 sensors, placed in the two transverse locations. The detail is provided below.

6.3.1 Midspan Location

- 15 strain gauges on the bottom of each DU (SGB1–15)
- 15 strain gauges on the top of each DU (SGT1–15)
- 15 string potentiometers attached to the bottom of each DU (SP1–15)
- 10 proximity probes placed between adjacent DUs (PP1–10)
- 1 temperature sensor placed on one kerb.

6.3.2 Quarterspan Location

- 8 strain gauges, placed on the bottom of every second DU (SGB16–23)
- 8 strain gauges, placed on the top of each DU (SGT16–23)
- 15 string potentiometers attached to the bottom of each DU (SP16–30).

It is noted that the top strain gauges, i.e. SGT1–15 and SGT16–23, were installed after removal of the DWS. The DWS was milled only prior to the load tests.

Figure 6.2: Stages of TSB severing in span 9

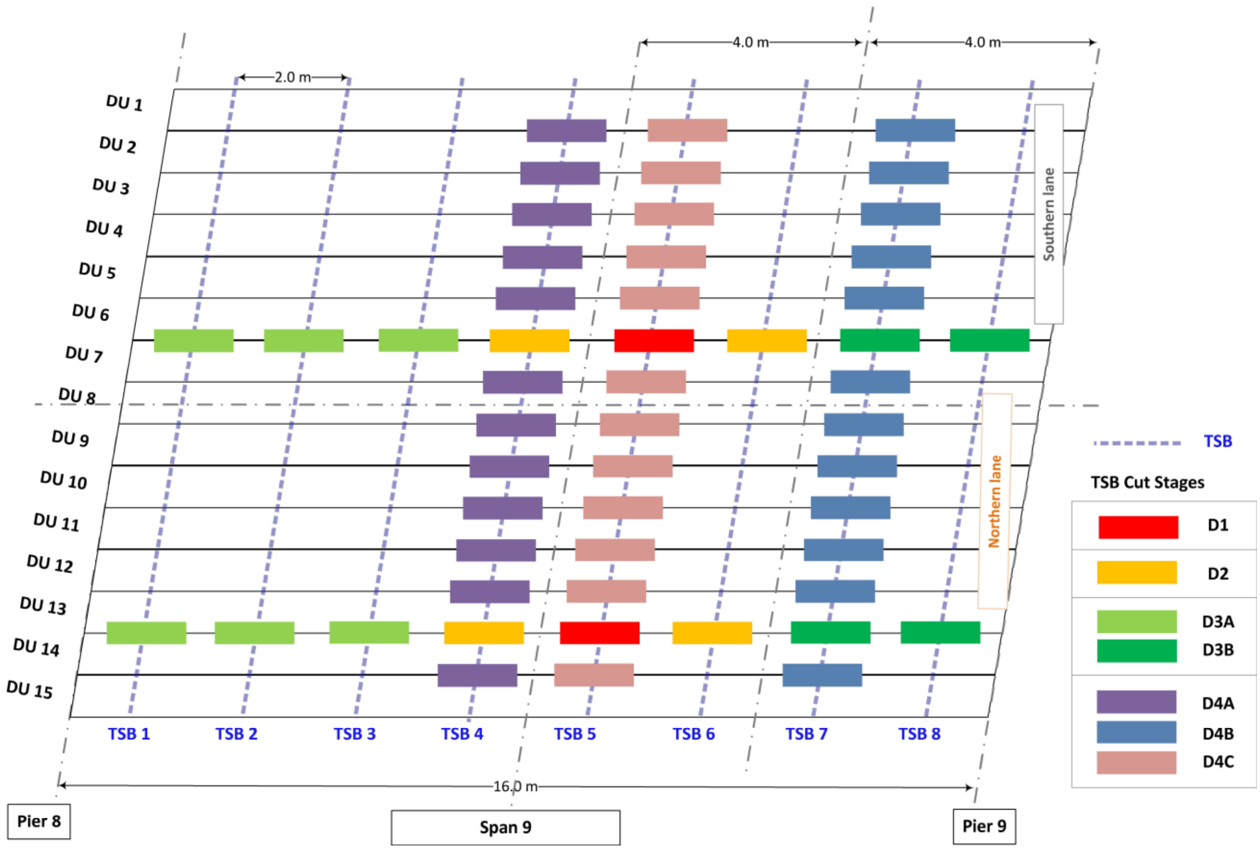

Note: The solid rectangles indicate the locations of each TSB cut.

Figure 6.3: Sensor arrangement

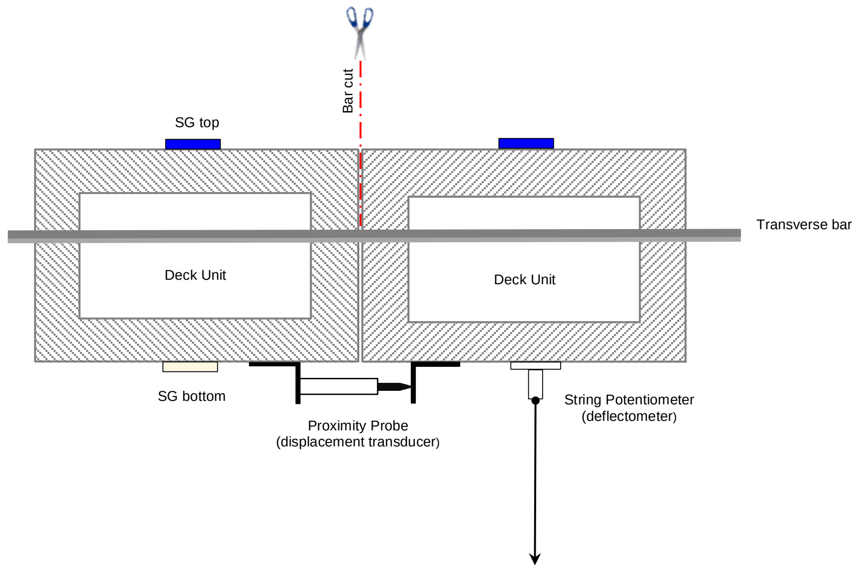

Note: Diagram showing the sensor layout at the cross-section of internal adjacent DUs.

6.4 Results

6.4.1 Performance of the Bridge in Operation

The measurements from the monitoring procedure provide the benchmarks of the bridge performance under operational traffic. The findings are summarised as follows:

- The maximum tensile strain measured under random traffic is 43 με. According to the linear strain-load relationship derived from the D0 load tests, ε = 43 με corresponds to an equivalent static load of 68 t, or a 50 t travelling vehicle with a DLA of 1.35. Strain values above 40 με were measured both within and outside peak hours.
- The maximum LDF derived from traffic events is 11.15%. Daytime and night-time traffic can be characterised by lower (8.0–9.0%) and higher (9.0–11.0%) LDF values, respectively. Higher LDFs are associated with traffic positioned on a single lane only (Figure 6.4).
- Most of the heavy traffic (which induced strain higher than 25 με) was localised on the southern lane (i.e. carried by DU1–8), and peaked at 4:30 pm on weekdays, when the structure sustained strains between 25 and 35 με, about 10 times per minute.

6.4.2 Performance of the Bridge before and after Incremental TSB Damage

Data from the load tests led to the following results:

- The maximum tensile strain measured in the undamaged state under the 82.5 t test vehicle is 54 με. The maximum deflection in the undamaged state is 3.5 mm, as measured under the 82.5 t test vehicle.
- The maximum tensile strain measured during the last damaged stage (D4C) is 50 µε (Figure 6.5). This value is 32% greater than the strain measured under equivalent load in the undamaged state (D0 2).
- The maximum LDF measured is 11.10% in the last damaged stage (D4C). The LDF increases by 18% from the undamaged stage to the last stage of TSB severing (Figure 6.5). The LDF increase is evident only when the TSB severing is carried out in several longitudinal locations (D3A).
- The NA position is lowered with incremental TSB severing. The maximum downward change of the NA position corresponds to an 18% reduction of the initial NA height, as measured from the bottom fibre.
- The maximum measured deflection is δ_{max} = 3.5 mm in stage D4C for DU7, which is 30±8% greater than the corresponding maximum deflection measured in the undamaged state (Figure 6.6). The theoretical prediction of the maximum deflection, δ'_{max}, as estimated by TMR via numerical models, in the last damaged stage (D4C) is δ'_{max} = 16.3 mm, i.e. appropriately 5 times larger than the actual measurement.
- The maximum gap opening reached 0.45 mm in stage D4B between DU6 and DU7, while the gap opening is estimated at 120 μm in D0 2 (Figure 6.6).

Figure 6.4: LDF distribution – over the 24-hour cycle of a weekday (Thursday)

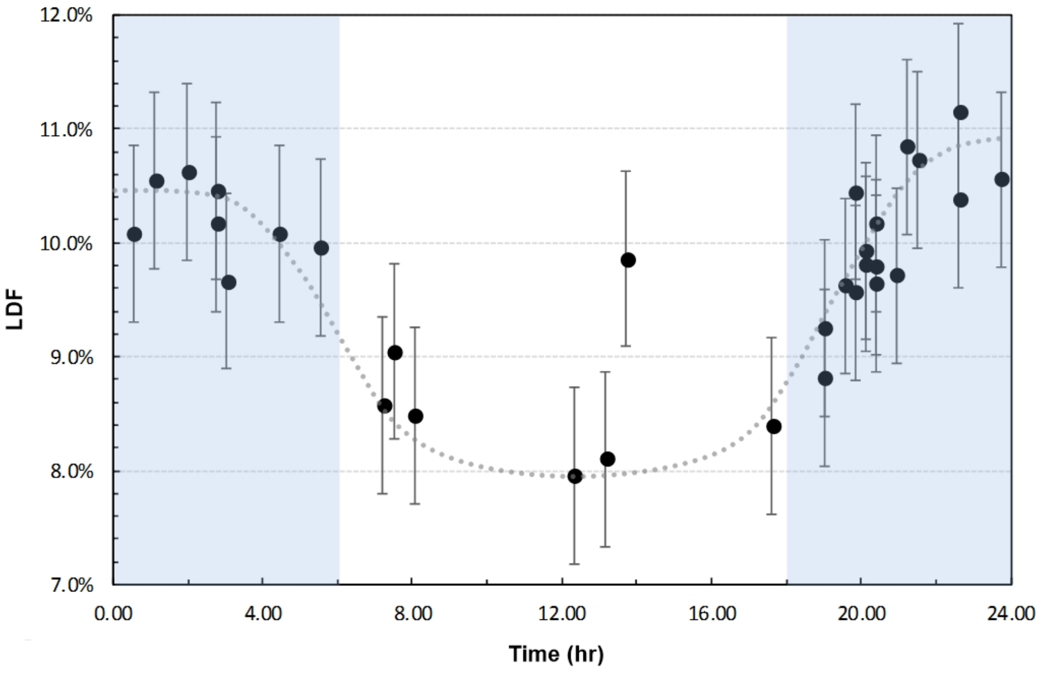

Note: Lower LDF values are associated with heavier traffic, i.e. when the traffic is positioned on both lanes.

Figure 6.5: LDF and strain distribution with increasing TSB damage

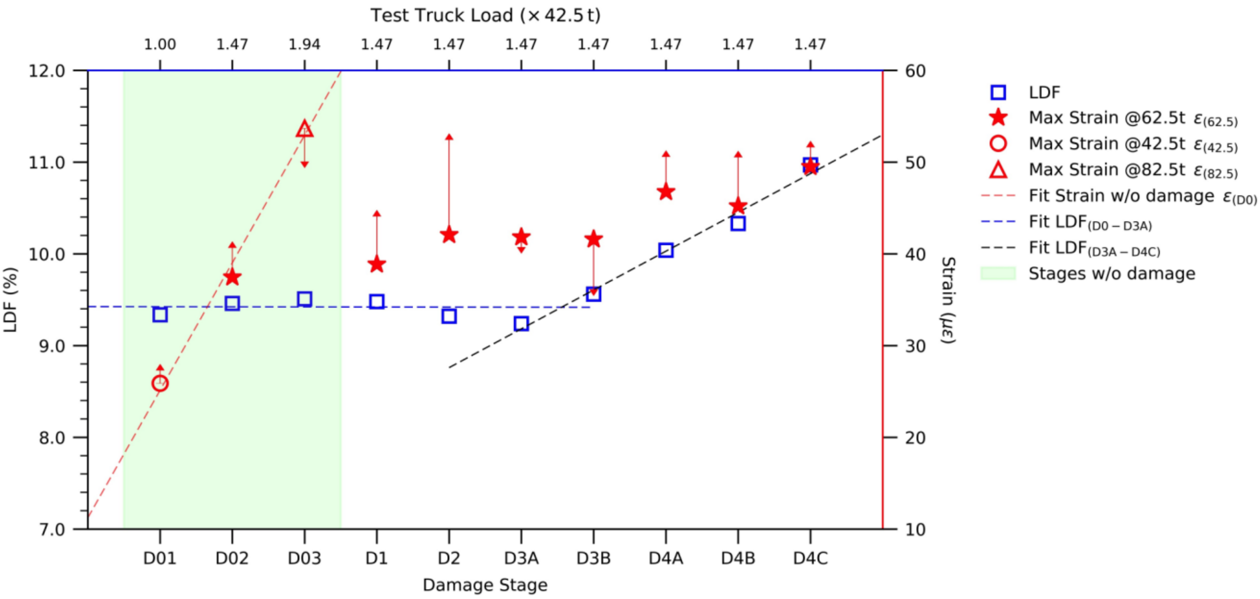

Note: For consistency, all considered tests are carried out with the RMS test truck running along the central path. D0 identifies the undamaged stage, as tested with the 42.5 t (D0 1), 62.5 t (D0 2), and 82.5 t loaded vehicle (D0 3).

Figure 6.6: DU movement variation with increasing TSB damage

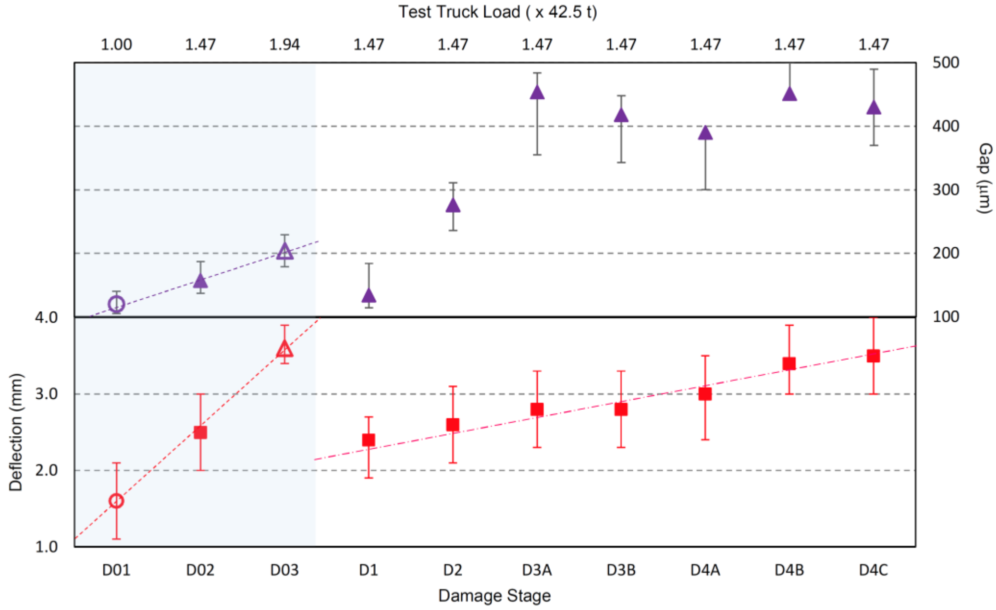

Note: Maximum DU movements derived in midspan from tests carried out with the RMS truck running along the central path.

6.4.3 Other Considerations

In light of the above results, the following remarks also apply:

- The maximum LDF associated with the deck response after comprehensive TSB severing (D4C) matches the maximum LDF measured under random traffic, i.e. when the deck was in the undamaged condition.
- The maximum tensile strain measured during in-service monitoring matches the maximum tensile strains measured after four stages of TSB severing, i.e. up to stage D3B.
- The most loaded DUs, after extensive TSB severing (D4C), carried 20% more load than in the undamaged stage.
- Based on the NA position variation, the severing of TSBs likely led to an 18% reduction of the load-bearing capacity of the overall superstructure.

7 CONCLUSIONS

The results from the research program consistently show that the performance of DU bridges exceeds theoretical expectations. The key findings are summarised below.

7.1 Performance at Serviceability and Elastic Limits

1. The laboratory tests have shown that the 8.3-m long reconstructed deck behaves elastically up to an applied load of 250 kN. The elastic upper limit corresponds to DU tensile and compressive strains of 170 $\mu\varepsilon$. The associated elastic deflections are within 2.8 mm (KU) and 4.2 mm (DU1–4).
2. Load testing of individual DUs and KUs, of the same design era and geometry, shows that the elastic limits were reached with an applied load of 110 kN for both KU and DU.
3. Short-term monitoring and load testing at serviceability of the Canal Creek Bridge, i.e. a DU bridge of similar span length (8.3 m) and geometry, located on a heavy vehicle route, show that the maximum tensile strain is 100 $\mu\varepsilon$, while the maximum measured deflection is 3.3 mm.
4. On the 16-m long span 9 of the Sandgate Rd Bridge, prior to TSB severing, maximum deflections of 2.5 mm and 3.5 mm were measured under the 62.5 t and 82.5 t test vehicles, respectively. The maximum strain of 54 $\mu\varepsilon$ was measured under the 82.5 t test vehicle, while maximum tensile strains of 43 $\mu\varepsilon$ were measured under operational traffic.
5. As measured in the laboratory, the relative movements at the joints between adjacent DUs reached 23 μm at the limit of the elastic range. On the other hand, joint gaps up to 0.14 mm were measured on the Canal Creek Bridge under a 48 t static crane. Static tests on the Sandgate Rd Bridge, prior to TSB damage, yielded maximum joint gaps of 0.12 and 0.20 mm, under the 62.5 t and 82.5 t vehicle, respectively.

7.2 Failure Modes and Ultimate State Limits

1. The laboratory tests carried out both on individual units and the assembled deck provided evidence of highly ductile behaviour of DUs up to failure.
2. The partial DU bridge failed in bending at 1040 kN, with KU cracking followed by the ductile failure of the DUs (Figure 5.4). Extensive flexural cracking of the KU started with 10 mm deflections, while extensive transverse cracking of the DUs was associated with 15 mm deflections. Prior to collapse of the test deck, ultimate deflections of 40 mm were measured for the KU, while the DU deflections reached 90 mm.
3. Ultimate deflections much larger than those measured for the partial DU bridge were reached in the tests of 9.1-m long individual units. In particular, individual KUs showed a failure mechanism controlled by the concrete, while a consistent ductile behaviour, i.e. with a clear yielding point, was displayed by individual DUs (Figure 4.3 to Figure 4.6).

7.3 Load Distribution Factors

1. Despite the differences in the units used for laboratory tests and in the bridges selected for site testing, the LDFs derived for the DUs were consistently around an average of 10%, with the highest values at 12–14%.
2. Higher DU LDF values were reached either at lower load levels (Figure 5.5 and Figure 6.4) or defective beam connections due to extensive TSB severing (Figure 6.5).

3. When the deck included the stiffer KUs, like in the Canal Creek Bridge and the partial DU bridge tested in the laboratory, higher LDF values were associated with these units. In the partial DU bridge, LDF values up to 39% were derived for the KU (Figure 5.5).

7.4 Effects of TSB Damage

1. The results from the tests carried out with incremental TSB severing (Section 6) show that extensive damage of the transverse bars does not result in the failure of the load transfer mechanism.
2. An LDF increase of 18% was measured from the undamaged to the last damaged stage of the TSBs (Figure 6.5). This was measured in combination with a 32% strain increase and a 30% increase of the maximum deflection.
3. Based on the NA position variation, the severing of the TSBs likely led to an 18% reduction of the load-carrying capacity of the overall superstructure.

7.5 Material Properties

1. The material tests carried out on cores from both the individual beams and the partial DU bridge indicated stronger materials than expected and commonly assumed for structural assessment of DU bridges.
2. The material tests carried out on the concrete cores from the individual 9.1 m units yielded a characteristic cylindrical strength 65 MPa for the DUs and 60 MPa for the KUs. On the other hand, the prestressed cable strength f'_p = 1620 MPa matched the design specifications.
3. While noting that the number of concrete samples from the 8.3 m long test deck was insufficient to apply basic sample statistics, the related concrete tests yielded f'_c = 53–64 MPa for the DUs, and f'_c = 69 MPa for the KU. For the maximum tensile stresses measured in the prestressing cables, 1848 MPa was derived for the DUs and 1802 for the KU. The average prestress loss was measured at 37% for DUs and 40% for the KU. All these values are significantly higher than design specifications and what are normally assumed for theoretical estimates. The steel reinforcement was tested for a 460 MPa yield strength, while the ultimate strength was measured at 548 MPa.

7.6 Measurements vs Theoretical Estimates

1. It is noted that the predicted deflections of the tested structures, as derived by TMR in accordance with relevant guidelines (Section 2.2), greatly exceed the measurements.
2. In particular, the estimated deflections were at least five times larger than those measured under given loads in both the Canal Creek Bridge and the Sandgate Rd Bridge.
3. Further, the deflections measured on the Sandgate Rd Bridge under increasing TSB damage did not match the predicted progression. As in Figure 6.6, an overall 30±8% increase of the deflections was measured between the undamaged stage and the last stage of TSB severing, while a net 76% increase was predicted. In the specific case of the 62.5 t test truck running along the central path, the maximum deflections were estimated at 9.5 mm in the undamaged stage and up to 16.3 mm in the last damaged stage.
4. In light of the above, the results from the research program provide crucial feedback and a comprehensive set of data to improve the numerical methods used for the assessment of DU bridges, as well as to calibrate the existing grillage models used by TMR for load rating of this bridge type.

8 RECOMMENDATIONS

The following recommendations are made:

- It was derived from this project that DU bridges generally perform significantly better than theoretically estimated using the current assessment methodology. However, until a verified theoretical method is available for the capacity assessment of this type of bridge, proof load testing is recommended to determine the actual capacity of a specific DU bridge.
- Use of field data in calibrating computer models should take into account the bridge-specific parameters.
- Further controlled load testing is required on DU bridges to provide a complete coverage of different span length, design era, substructure type and configuration, and site-specific conditions, etc. so that the findings can be generalised to the whole network.
- For material strength tests, since the number of testing samples is limited, the test results may not necessary be representative. Further material tests are required before using the measured material strength in the assessment and rating of existing structures.

REFERENCES

AASHTO 2014, *AASHTO LRFD bridge design specifications*, LRFDUS-7, American Association of State Highway and Transportation Officials, Washington, DC, USA.

American Concrete Institute 2008, *Building code requirements for structural concrete*, ACI 318-08, ACI, Farmington Hills, Michigan, USA.

Badwan, I & Liang, RY 2007, 'Transverse post-tensioning design of precast concrete multibeam deck', *PCI Journal*, vol. 52, no. 4, pp. 84-92.

Buckle, IG 1984, *Methods of analysis of multi-beam bridges*, Road Research Unit bulletin no. 72, National Roads Board, Wellington, New Zealand.

Fu, CC, Pan, Z & Ahmed, MS 2011, 'Transverse posttensioning design of adjacent precast solid multibeam bridges', *Journal of Performance of Constructed Facilities*, vol. 25, no. 3, pp. 223-30.

Hambly, EC 1991, *Bridge deck behaviour*, 2nd edn, CRC Press, Boca Raton, Florida, USA.

Hulsbos, CL 1962, 'Lateral distribution of load in multibeam bridges', *Highway Research Board Bulletin,* no. 339, pp. 67-79.

Kohnke, P (ed) 1999, *ANSYS theory reference,* 11th edn, ANSYS, Canonsburg, PA, USA.

Ngo, H, Kotze, R & Pape, T 2014, 'S3: Deck unit bridge deck analysis under live load: year 1 report', contract report, ARRB Group, Vermont South, Vic.

Ngo, H & Pape, T 2015, 'BIS 7703 Canal Creek bridge: load test and in-service monitoring', contract report RC8286, ARRB Group, Vermont South, Vic.

Ngo, H, Pape, T & Kotze, R 2016, '*S3:* Deck unit bridge deck analysis under live load: year 2 report', contract report RC007205, ARRB Group, Vermont South, Vic.

Ngo, H 2017, 'S3: Deck unit bridge deck analysis under live load: year 3 report', contract report RC010575, ARRB Group, Vermont South, Vic.

Ngo, H & Zanardo, G 2017, 'GUN – Sandgate Road Bridge load testing report', contract report, RC16022, under review, ARRB Group, Vermont South, Vic.

Queensland Department of Transport and Main Roads 2013, *Annexure S02: Modelling deck unit bridge superstructures for Tier 1 assessments*, rev no. 1.04, TMR, Brisbane, Qld.

West, R 1973, *Recommendations on the use of grillage analysis for slab and pseudo-slab bridge decks*, Cement and Concrete Association, London, UK.